Relativistic Quantum Chaos: Neutrino Billiards

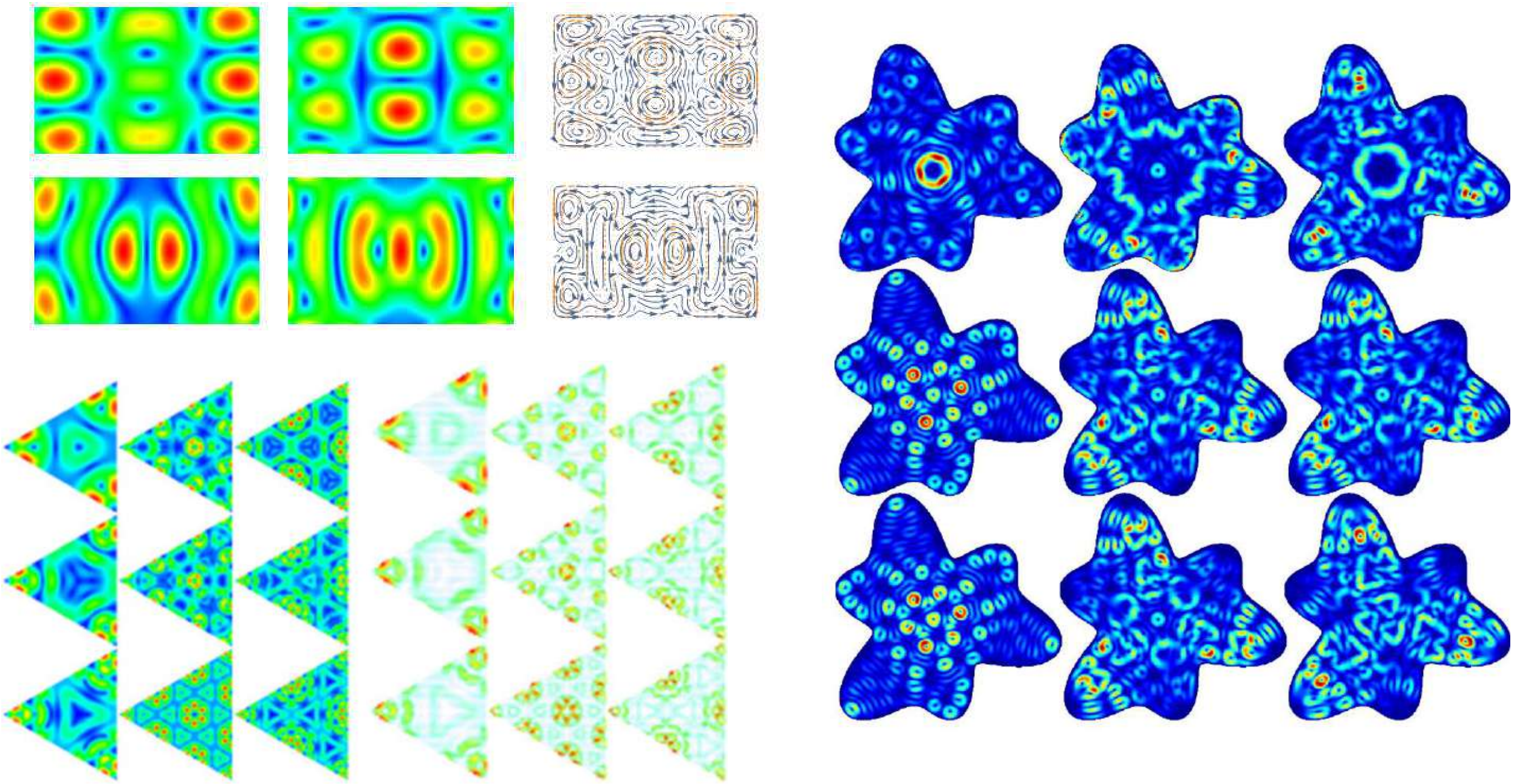

Central Conjectures of Quantum Chaos

- Nonrelativistic Quantum Systems / Quantum Billiards
- Berry-Tabor Conjecture:
  The spectral fluctuation properties of generic integrable systems coincide with those of uncorrelated random numbers from a Poisson process
- Bohigas-Gianonni-Schmit Conjecture (1984) [Berry (1977), Casati et al. (1980)]:
  The spectral fluctuation properties of generic classically chaotic systems coincide with those of random matrices from the Gaussian Ensembles
- Relativistic Quantum Systems / Quantum Billiards

→ Question: Do the conjectures apply to relativistic quantum billiards like neutrino billiards?
→ Problem: NBs do not have a well-defined classical limit
→ We use the semiclassical approach (length spectra, Husimi distributions)

Graphene

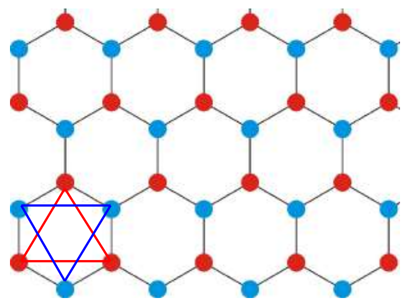

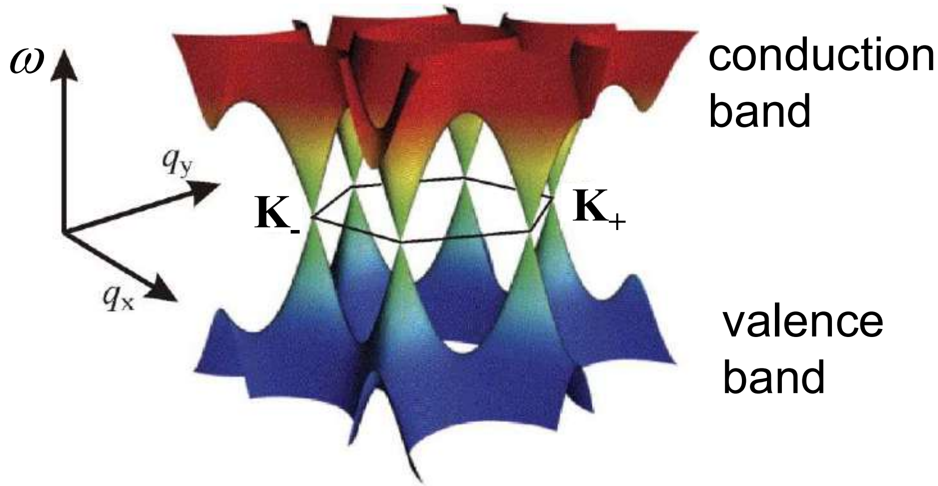

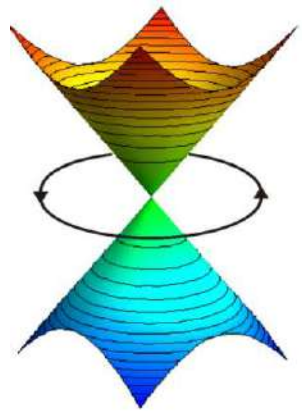

- Near each corner of the first hexagonal Brillouin zone the electron energy ω exhibits a linear dependence on the quasimomentum q
- Close to the diabolical ('Dirac') points the band structure is described by the Dirac equation of massless fermions

$$\pm \begin{pmatrix} 0 & \partial_x - i\partial_y \\ \partial_x + i\partial_y & 0 \end{pmatrix} \begin{pmatrix} \Psi_A \\ \Psi_B \end{pmatrix} = i\frac{\omega - \omega_D}{v_F} \begin{pmatrix} \Psi_A \\ \Psi_B \end{pmatrix}$$

- Independent contributions from K_+ and K_- valleys $\Rightarrow$ 4D Dirac equation

Graphene Billiards

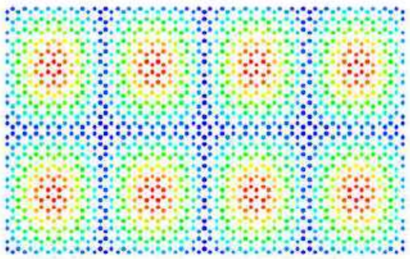

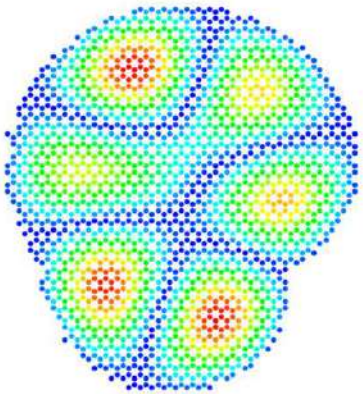

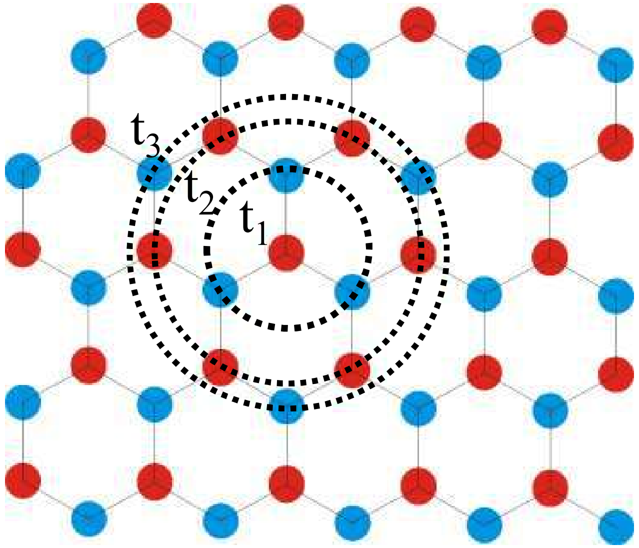

- Tight-binding model

$$\hat{\mathcal{H}}_{ij}^{TBM} = t_0\delta_{ij} + t_1\delta(|\boldsymbol{r}_i - \boldsymbol{r}_j| - d_0) + t_2\hat{\delta}(|\boldsymbol{r}_i - \boldsymbol{r}_j| - d_1) + \ldots..$$

- Assumption: interaction of the graphene p_z orbitals non-negligible for 1st, 2nd and 3rd nearest neighbors
- Graphene billiard: Dirichlet BCs along the 1st missing row of atoms outside sheet

DOS of Rectangular and Africa-Shaped GBs

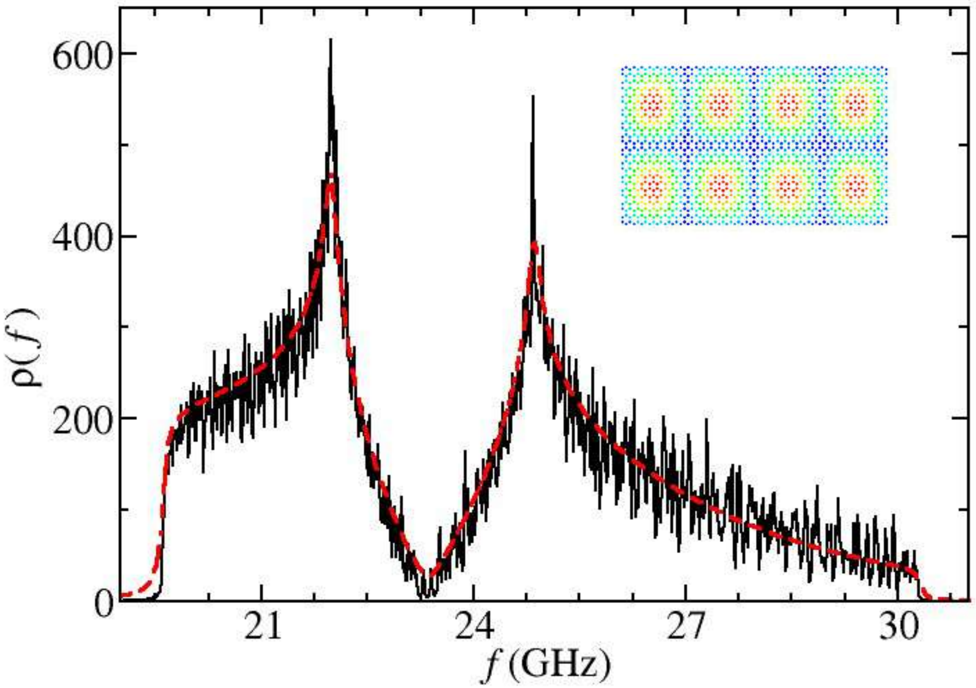

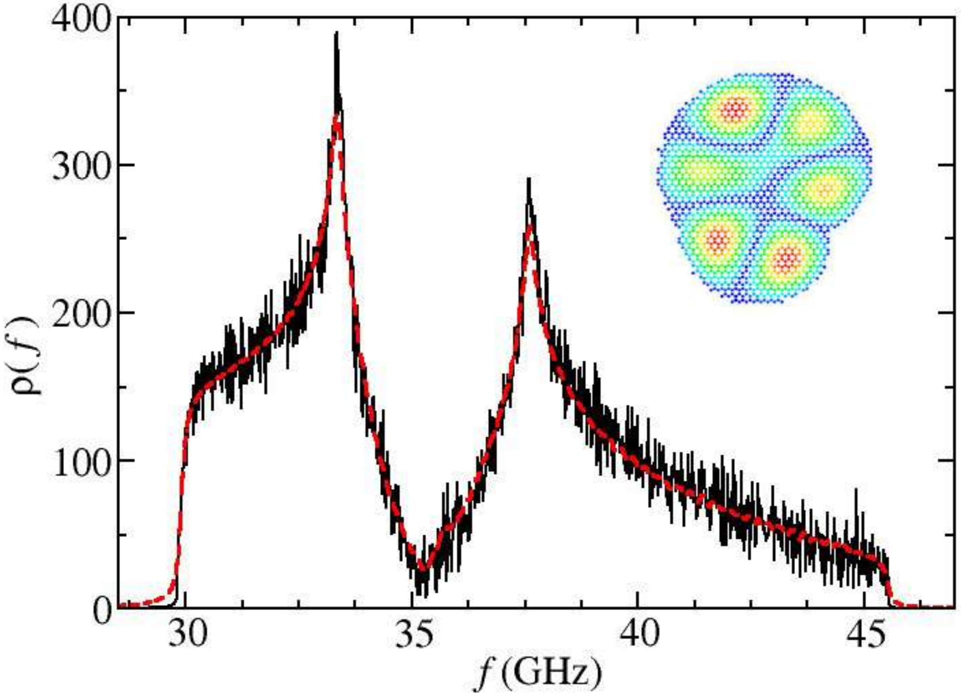

Ratio Distributions for Dirac / Graphene Billiards

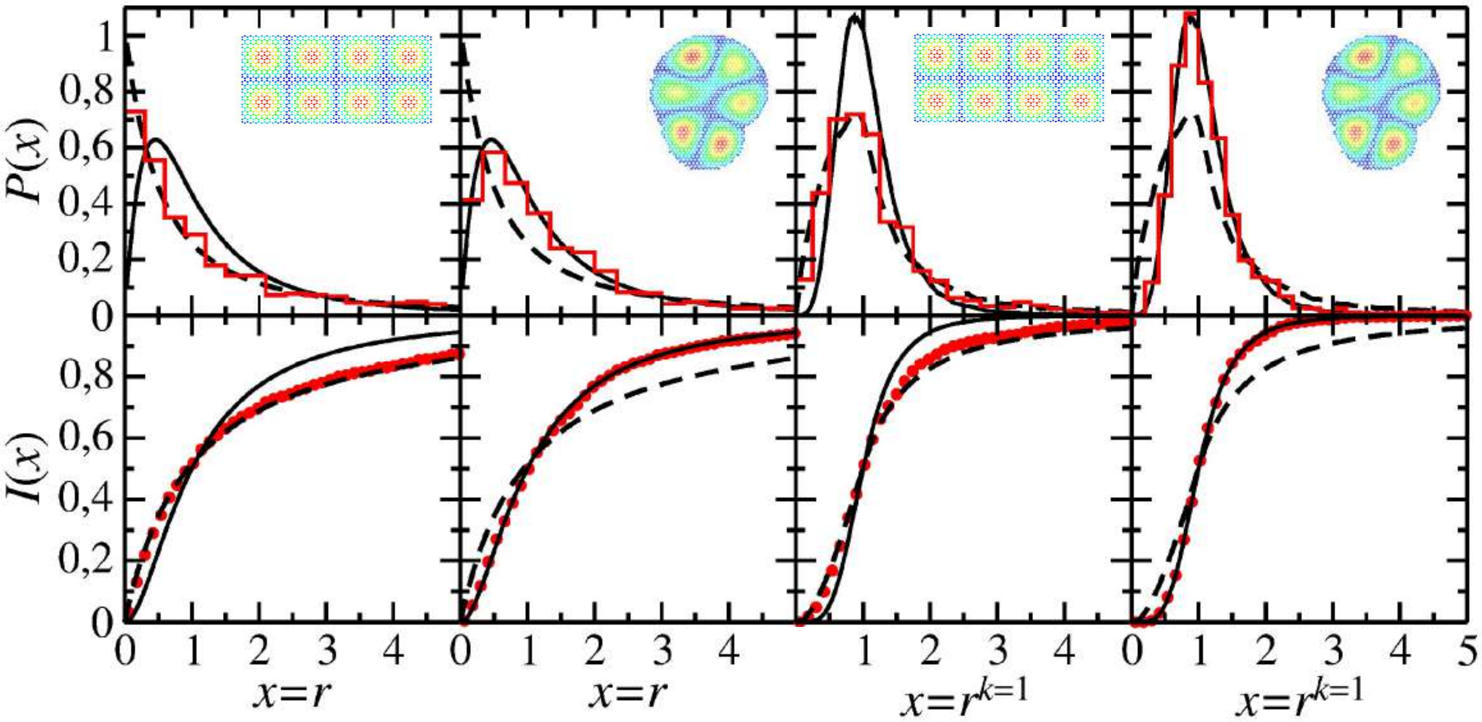

- Ratio distribution of all 1656 (1823) resonance frequencies of rectangular (Africa) billiard agrees with Poisson (GOE)
- The same holds for the (k=1)-overlapping ratio distribution

Massless Spin-1/2 Particle in a Potential

Proc. R. Soc. Lond. A **412**, 53–74 (1987)
Printed in Great Britain

Neutrino billiards: time-reversal symmetry-breaking without magnetic fields

BY M. V. BERRY, F.R.S., AND R. J. MONDRAGON
H. H. Wills Physics Laboratory, Tyndall Avenue, Bristol BS8 1TL, U.K.

- Dirac equation

$$\begin{pmatrix} V & -i\hbar(\partial_x - i\partial_y) \\ -i\hbar(\partial_x + i\partial_y) & -V \end{pmatrix} \begin{pmatrix} \psi_1(\boldsymbol{r}) \\ \psi_2(\boldsymbol{r}) \end{pmatrix} = k \begin{pmatrix} \psi_1(\boldsymbol{r}) \\ \psi_2(\boldsymbol{r}) \end{pmatrix}$$

- For $V \neq 0$ the Dirac Hamiltonian is not invariant under $\hat{\mathrm{T}} = i\hat{\sigma}_y \hat{\mathrm{K}}$

→ chaotic systems with no geometric symmetries follow GUE statistics

Dirac Equation for Neutrino Billiards

Berry & Mondragon, Proc. R. Soc. Lond. A 412, 53 (1987)

- Dirac equation for a free spin-$1/2$ particle with mass m

$$\hat{H}_D \boldsymbol{\psi} = \left(c\hat{\boldsymbol{\sigma}} \cdot \hat{\mathbf{p}} + mc^2 \hat{\boldsymbol{\sigma}}_{\boldsymbol{z}}\right) \boldsymbol{\psi} = E\boldsymbol{\psi},\ \boldsymbol{\psi} = \begin{pmatrix} \psi_1 \\ \psi_2 \end{pmatrix}$$

- BC requires that the outward current vanishes along boundary

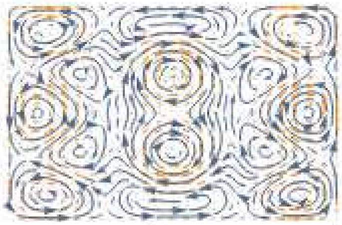

$$\mathbf{n} \cdot \left[\boldsymbol{\psi}^\dagger \boldsymbol{\nabla}_{\boldsymbol{p}} \hat{\boldsymbol{H}}_D \boldsymbol{\psi}\right] = 0$$

- BC links the spinor components at the boundary

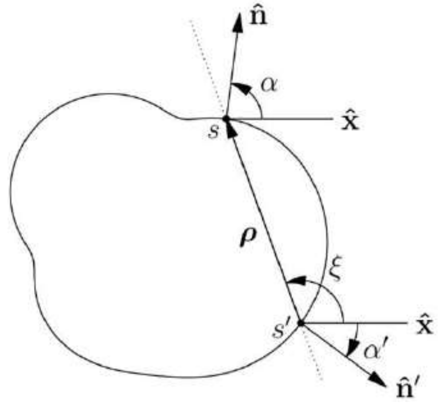

$$\psi_2(s) = ie^{i\alpha(s)}\psi_1(s)$$

- Coordinates in the complex plane: $w(s) = x(s) + iy(s)$
- Normal vector: $\boldsymbol{n}(s) = [\cos\alpha(s), \sin\alpha(s)]$
- Polar coordinates: $x(r,\phi) + iy(r,\phi) = w(r,\phi) = R(r,\phi)e^{i\phi} \quad \phi \in [0, 2\pi),\ r = [0, r_0]$
- Parameter $\phi \rightarrow$ arc length: $s(\phi) = \int_0^\phi |w'(\tilde{\phi})|d\tilde{\phi},\ s \in [0, \mathcal{L})\,, ds = |w'(\phi)|d\phi$

Dirac Equation for Massive Neutrino Billiards

- The energy E is given in terms of the free space wavevector k as

$$E = \hbar c k_E = \hbar c k\sqrt{1+\beta^2},\ \beta = \frac{mc}{\hbar k}$$

- The nonrelativistic limit $k\beta \to \infty$ complies with the BC
- Define

$$\psi = \begin{pmatrix} \sqrt{\frac{1+\sin\theta_\beta}{2}}\tilde{\psi}_1 \\ \sqrt{\frac{1-\sin\theta_\beta}{2}}\tilde{\psi}_2 \end{pmatrix}$$ with $\sin\theta_\beta = \frac{\beta}{\sqrt{1+\beta^2}}$.

nonrel. Limit $\Leftrightarrow$ $\theta_\beta \to \pi/2$
ultrarel. Limit $\Leftrightarrow$ $\theta_\beta \to 0$

$\Rightarrow$ $k\tilde{\boldsymbol{\psi}}(\boldsymbol{r}) + i\hat{\boldsymbol{\sigma}}\cdot\nabla\tilde{\boldsymbol{\psi}}(\boldsymbol{r}) = 0$ with $\tilde{\psi}_2(s) = ie^{i\alpha(s)}\mathcal{K}^{-1}\tilde{\psi}_1(s)$ $\quad \mathcal{K} = \sqrt{\frac{1-\sin\theta_\beta}{1+\sin\theta_\beta}}$

- The resulting Dirac equation has the same form as for the NB with m=0
- For $m \to 0$ the Dirac Hamiltonian is not time-reversal invariant

$\Rightarrow$ if it's shape corresponds to that of a chaotic billiard, GUE is expected
- For $m \to \infty$ we have $\psi_2 \to 0$ and the BC for ψ_1 becomes Dirichlet

Boundary Integral Equation for NBs

- Combining the Dirac equation and the matrix equation satisfied by the associated free-space Green function yields the boundary integral

$$2i \oint_{\partial\Omega} \mathrm{d}s\, \boldsymbol{n} \cdot \left[\psi(\boldsymbol{r})^\dagger \hat{\boldsymbol{\sigma}} \hat{G}_0(\boldsymbol{r}, \boldsymbol{r}')\right] = \begin{cases} \psi^\dagger(\boldsymbol{r}') & , \ \boldsymbol{r}' \in \Omega \backslash \partial\Omega \\ \frac{1}{2}\psi^\dagger(\boldsymbol{r}') & , \ \boldsymbol{r}' \in \partial\Omega \\ 0 & , \ \text{otherwise} \end{cases}$$

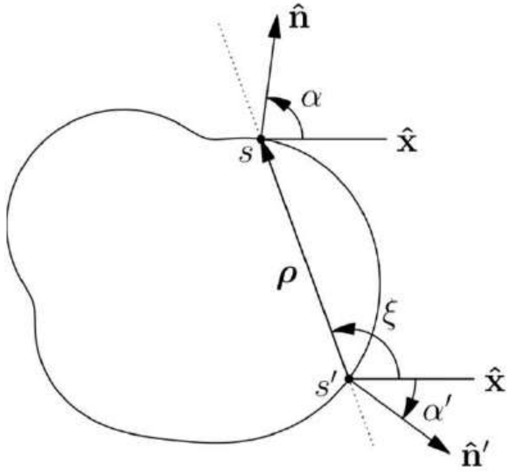

- Free-space Green function

$$G^0(\boldsymbol{r}, \boldsymbol{r}') = -\frac{1}{4}\begin{pmatrix} ik & \partial_x - i\partial_y \\ \partial_x + i\partial_y & ik \end{pmatrix} H_0^{(1)}(k|\boldsymbol{r} - \boldsymbol{r}'|).$$

- Incorporate the B.C. in the equation for $\boldsymbol{r}' \in \partial\Omega$

$$\tilde{\psi}_1^*(\phi') = \frac{ik}{2}\oint_{\partial\Omega} |w'(\phi)| d\phi \tilde{\psi}_1^*(\phi) \left\{-\mathcal{K}^{-1} H_0^{(1)}[k\rho(\phi,\phi')] + e^{-i\alpha(\phi)} e^{i\xi(\phi,\phi')} H_1^{(1)}[k\rho(\phi,\phi')]\right\}$$

$$\tilde{\psi}_2^*(\phi') = \frac{ik}{2}\oint_{\partial\Omega} |w'(\phi)| d\phi \tilde{\psi}_2^*(\phi) \left\{\mathcal{K} H_0^{(1)}[k\rho(\phi,\phi')] + e^{i\alpha(\phi)} e^{-i\xi(\phi,\phi')} H_1^{(1)}[k\rho(\phi,\phi')]\right\}$$

$$e^{i\xi(\phi,\phi')} = \frac{w(\phi) - w(\phi')}{|w(\phi) - w(\phi')|}, \ \rho(\phi,\phi') = |w(\phi) - w(\phi')|$$

- H_0 and H_1 have singularities at $\rho = 0$

Boundary Integral Method for Massive NBs
Dietz & Li, PRE 102, 042214 (2020)

- For $m=0$ the singularities are removed with the replacements

$$\Phi_1(n,s) = \left\{\psi_1(n,s) + [-ie^{-i\alpha(s)}]\psi_2(n,s)\right\}/2$$
$$\Phi_2(n,s) = \left\{\psi_2(n,s) + [ie^{i\alpha(s)}]\psi_1(n,s)\right\}/2,$$

$$\Phi_{1,2}(n,s) \xrightarrow{n\to 0^-} \psi_{1,2}(s)$$

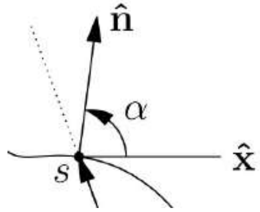

in coordinates (n,s) normal / tangential to boundary, and with the relation

$$\oint_{\partial\Omega} ds e^{i\frac{\Delta\Phi(s,s')}{2}} \tilde{\psi}_1^*(s)\cos\left(\frac{\Delta\Phi(s,s')}{2}\right)\frac{ik}{4}H_0^{(1)}(k\rho) = \oint_{\partial\Omega} ds e^{i\frac{\Delta\Phi(s,s')}{2}} i\tilde{\psi}_1^*(s)$$
$$\times\left[\sin\theta_\beta \sin\left(\frac{\Delta\Phi(s,s')}{2}\right)\frac{ik}{4}H_0^{(1)}(k\rho) - \cos\theta_\beta \sin\left(\frac{\alpha(s')+\alpha(s)}{2} - \xi(s,s')\right)\frac{ik}{4}H_1^{(1)}(k\rho)\right]$$

- Boundary integral equation for the first spinor component

$$(1-\sin\theta_\beta)\,\tilde{\psi}_1^*(\phi') = \frac{ik}{4}\oint_0^{2\pi}|w'(\phi)|d\phi Q_k(\phi',\phi)\tilde{\psi}_1^*(\phi)$$

$$Q_k(\phi',\phi) = \cos\theta_\beta\left[e^{i(\alpha(\phi')-\alpha(\phi))} - 1\right]H_0^{(1)}(k\rho)$$
$$+\left\{[1-\sin\theta_\beta]\,e^{i(\xi(\phi,\phi')-\alpha(\phi))} + [1+\sin\theta_\beta]\,e^{-i(\xi(\phi,\phi')-\alpha(\phi'))}\right\}H_1^{(1)}(k\rho).$$

- In the integral $\phi=\phi'$ is excluded, as it is accounted for on the lhs

Spectral Properties of Half-Circle QB With Robin BCs

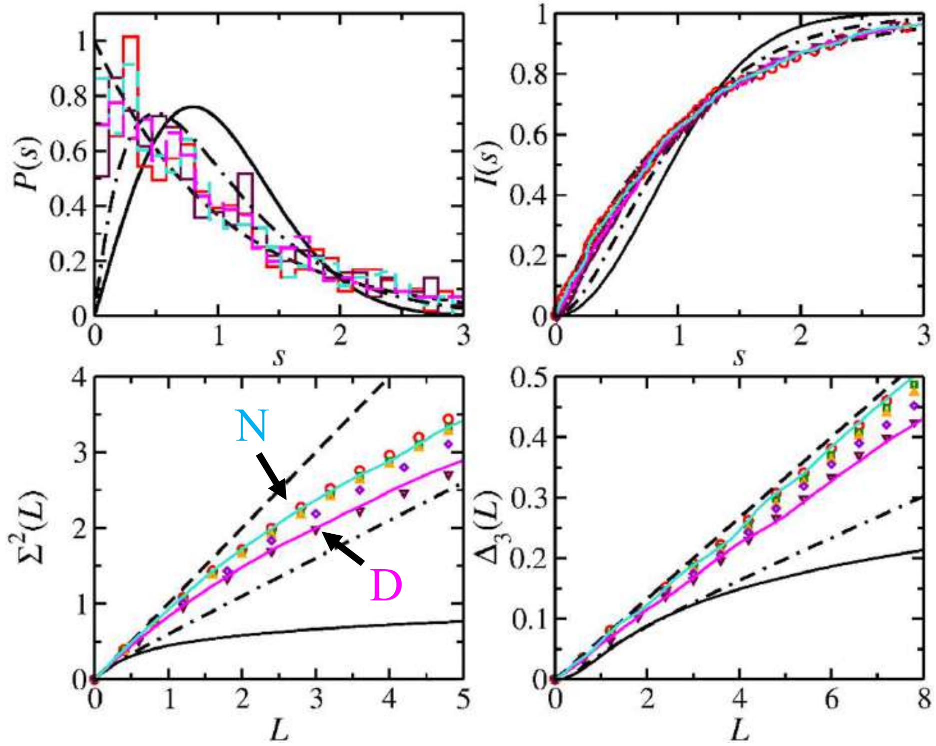

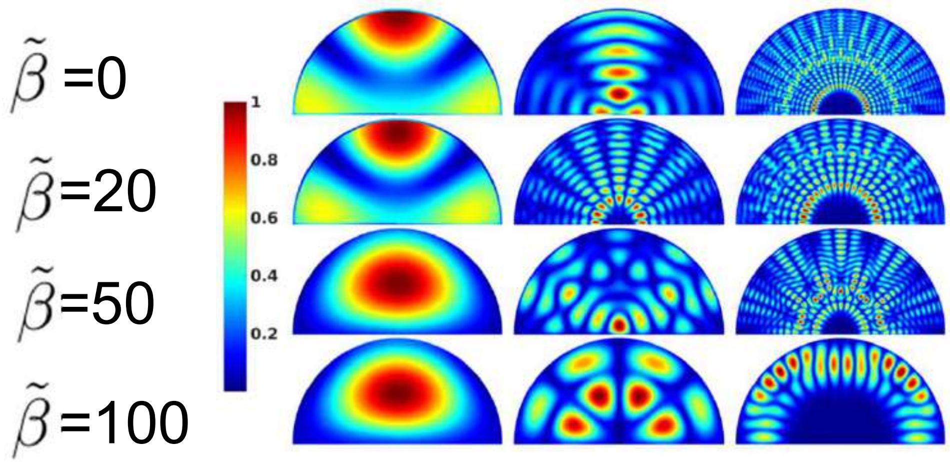

- Robin BC $\left[\tilde{\beta} + \frac{1}{2}\kappa(s)\right]\Phi_j(s) + \partial_n \Phi_j(n,s)\big|_{n\to 0^-} = 0 \quad \tilde{\beta} = \frac{mc}{\hbar}$

- Shown are results for the symmetric solutions

Trace Formula for the Spectral Density of Massive Neutrino Billiards

BD & Z. Li, PRE102, 042214 (2020)

- Quantization condition deduced from the BIEs for Massive NBs

$$\boldsymbol{u}(s') = \hat{\boldsymbol{Q}}(k)\boldsymbol{u}(s) \quad \Rightarrow \quad \det\left(\mathbb{1} - \hat{\boldsymbol{Q}}(k)\right) = 0 \quad \Rightarrow \quad \rho^{fluc}(k) = \frac{1}{\pi}\Im\sum_{p=1}^{\infty}\frac{1}{p}\frac{\mathrm{d}}{\mathrm{d}k}\left[\mathrm{Tr}\left(\hat{\boldsymbol{Q}}\right)^p(k)\right]$$

- Trace formula is a sum over the periodic orbits of the classical billiard

$$\Im\frac{1}{p}\frac{\mathrm{d}}{\mathrm{d}k}\left[\mathrm{Tr}\left(\hat{\boldsymbol{Q}}\right)^p(k)\right] = \Re\sum_{\gamma_p}\cos\left(\Phi_{\gamma_p} - p\frac{\pi}{2}\right)\mathcal{B}^{\tilde{\beta}}_{\gamma_p}e^{i\Gamma^{\tilde{\beta}}_{\gamma_p}}\mathcal{A}_{\gamma_p}e^{i\Theta_{\gamma_p}} + \Re\sum_{\gamma_p}\cos\left(\Phi_{\gamma_p} + p\frac{\pi}{2}\right)\tilde{\mathcal{B}}^{\tilde{\beta}}_{\gamma_p}e^{i\tilde{\Gamma}^{\tilde{\beta}}_{\gamma_p}}\mathcal{A}_{\gamma_p}e^{i\Theta_{\gamma_p}}$$

QB

$$\mathcal{A}_{\gamma_p} = \frac{l^{(p)}_{\mathrm{PO}}}{r_{\mathrm{PO}}\sqrt{|\mathrm{Tr}M^{(p)}_{\mathrm{PO}} - 2|}}$$

$$\Theta_{\gamma_p} = kl^{(p)}_{\mathrm{PO}} - \frac{\pi}{2}\mu^{(p)}_{\mathrm{PO}},$$

Gutzwiller

- The factor $\mathcal{B}^{(l)\tilde{\beta}}_{\gamma_p}e^{i\Gamma^{(l)}_{\gamma_p}}$ depends on m and the direction of propagation of the PO

$$\rho^{fluc}(k;\tilde{\beta}) \xrightarrow{\tilde{\beta}\to\infty} \frac{1}{\pi}\Re\sum_{\gamma_p}\mathcal{A}_{\gamma_p}e^{i\Theta_{\gamma_p}}$$

$$\rho^{fluc}(k;\tilde{\beta}) \xrightarrow{\tilde{\beta}\to 0} \frac{1}{\pi}\Re\sum_{\gamma_p}(-1)^p\cos\left(\Phi_{\gamma_p}\right)\cos\left(p\frac{\pi}{2}\right)\mathcal{A}_{\gamma_p}e^{i\Theta_{\gamma_p}} \quad \Rightarrow$$

Only POs with even # reflections p contribute

Wave Functions and Current for the Rectangular NB

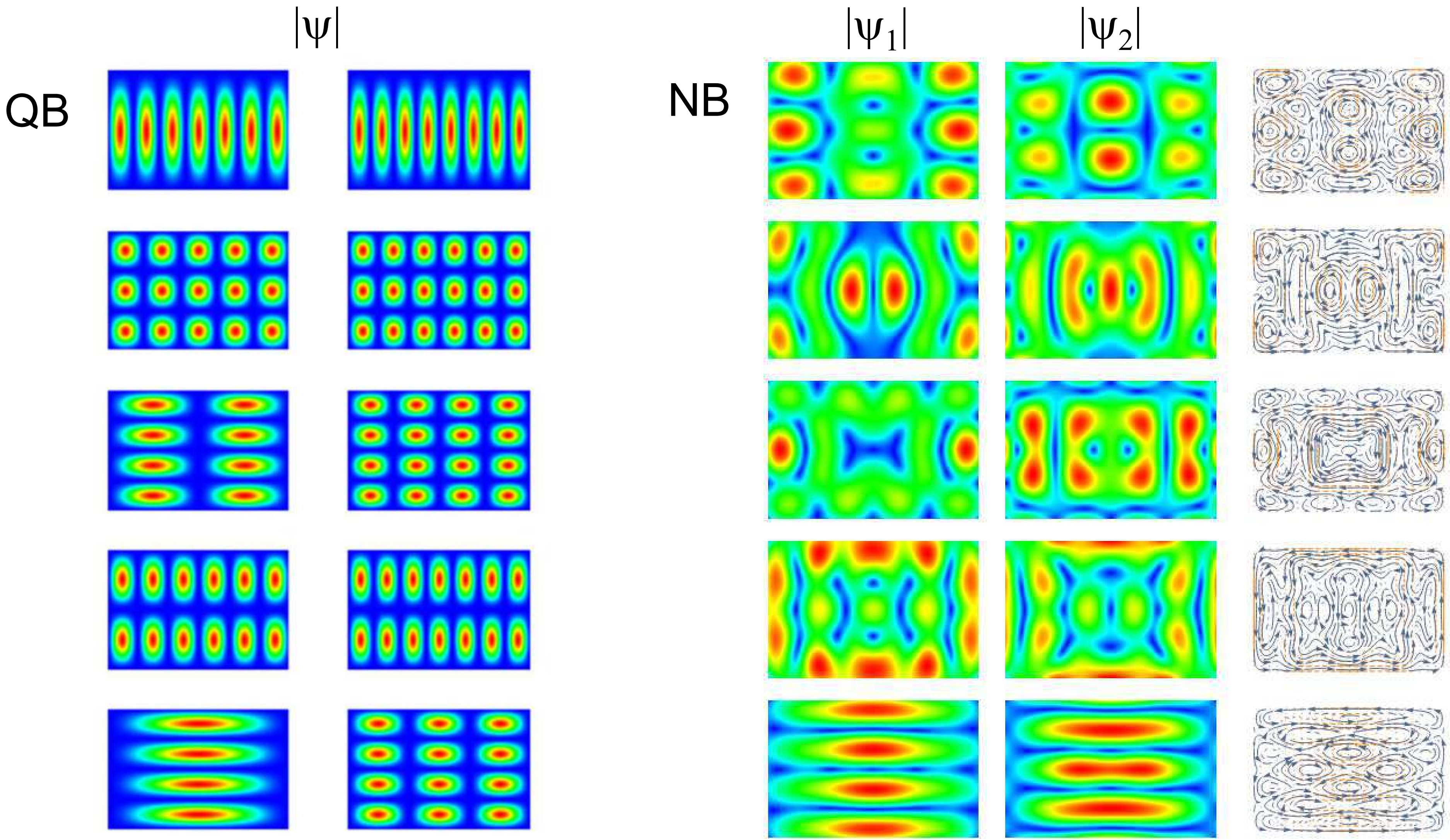

NBs with Shapes Exhibiting a Mirror Symmetry

- Coordinate (orthogonal) transformation $\Leftrightarrow$ unitary transformation in Dirac Hamiltonian

$$\boldsymbol{r}' = \hat{\boldsymbol{R}}\boldsymbol{r} \qquad \Rightarrow \qquad \hat{\boldsymbol{H}}_D(\boldsymbol{r}') = \hat{\boldsymbol{H}}'_D = \hat{\boldsymbol{U}}^\dagger \hat{\boldsymbol{H}}_D \hat{\boldsymbol{U}},\, \bar{\psi}(\boldsymbol{r}') = \hat{\boldsymbol{U}}^\dagger \tilde{\psi}(\boldsymbol{r})$$

- Reflection at the x- or y-axis

$$\hat{\boldsymbol{R}}_{x,y} = \pm\hat{\boldsymbol{\sigma}}_z \qquad \hat{\boldsymbol{H}}'_D = \hat{\boldsymbol{H}}_D(\hat{\boldsymbol{R}}_{x,y}\boldsymbol{r})$$

$$\hat{\boldsymbol{U}}_x = \hat{\boldsymbol{\sigma}}_x \qquad \bar{\psi}^{\boldsymbol{T}}_x(\boldsymbol{r}') = \left[\tilde{\psi}_2(\boldsymbol{r}), \tilde{\psi}_1(\boldsymbol{r})\right]$$

$$\hat{\boldsymbol{U}}_y = i\hat{\boldsymbol{\sigma}}_y \qquad \bar{\psi}^{\boldsymbol{T}}_y(\boldsymbol{r}') = \left[-\tilde{\psi}_2(\boldsymbol{r}), \tilde{\psi}_1(\boldsymbol{r})\right]$$

- The transformed spinor functions do not fulfill the boundary condition

$$\bar{\psi}_2(s) \neq ie^{i\bar{\alpha}(s)}\mathcal{K}^{-1}\bar{\psi}_1(s)$$

$\Rightarrow$ not classifiable according to their transformation properties under reflection at the mirror axis

- Reflection at the x- or y-axis of the Dirac equation yields

$$\hat{\boldsymbol{H}}_{NB}(-x,y) = \hat{\boldsymbol{H}}^\star_{NB}(x,y) \quad \Rightarrow \quad [\psi_1(-x,y), \psi_2(-x,y)] = \pm[\psi_1^\star(x,y), \psi_2^\star(x,y)]$$

$$\hat{\boldsymbol{H}}_{NB}(x,-y) = \hat{\boldsymbol{\sigma}}_{\boldsymbol{z}}\hat{\boldsymbol{H}}^\star_{NB}(x,y)\hat{\boldsymbol{\sigma}}_{\boldsymbol{z}} \Rightarrow [\psi_1(x,-y), \psi_2(x,-y)] = [\pm\psi_1^\star(x,y), \mp\psi_2^\star(x,y)]$$

Wave Functions and Currents of Elliptic NB

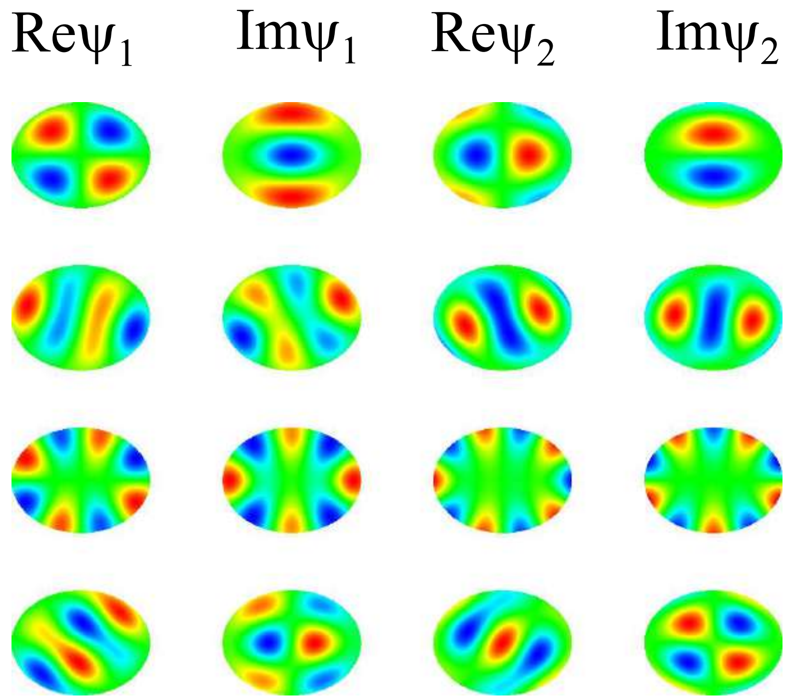

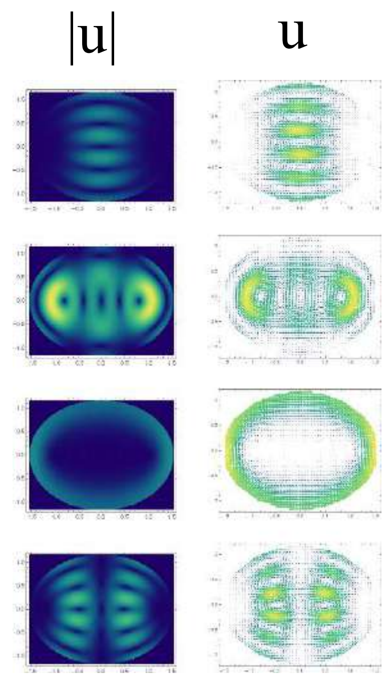

$$\hat{\boldsymbol{u}} = \boldsymbol{\nabla}_{\boldsymbol{p}} \hat{H}_D = c\hat{\boldsymbol{\sigma}},\ \boldsymbol{u}(\boldsymbol{r}) = c\psi^{\dagger}\hat{\boldsymbol{\sigma}}\psi$$

- The ellipse has a reflection symmetry with respect to the x- and y-axis
  $\Rightarrow$ it has a twofold symmetry
- All wave functions are either symmetric or antisymmetric with respect to rotation by π

NBs with Shapes with N-fold Rotational Symmetry

- Counterclockwise rotation by $2\pi/N$

$$\hat{\boldsymbol{R}}_N = \begin{pmatrix} \cos\left(\frac{2\pi}{N}\right) & -\sin\left(\frac{2\pi}{N}\right) \\ \sin\left(\frac{2\pi}{N}\right) & \cos\left(\frac{2\pi}{N}\right) \end{pmatrix} \qquad \hat{\boldsymbol{U}}_N = \begin{pmatrix} e^{i\frac{\pi}{N}} & 0 \\ 0 & e^{-i\frac{\pi}{N}} \end{pmatrix} \qquad \bar{\psi}(\boldsymbol{r}') = \begin{pmatrix} \bar{\psi}_1(\boldsymbol{r}') \\ \bar{\psi}_2(\boldsymbol{r}') \end{pmatrix} = \begin{pmatrix} e^{-i\frac{\pi}{N}}\tilde{\psi}_1(\boldsymbol{r}) \\ e^{i\frac{\pi}{N}}\tilde{\psi}_2(\boldsymbol{r}) \end{pmatrix}$$

- N-fold rotational symmetry: $w(s') = e^{i\frac{2\pi}{N}} w(s) \qquad e^{i\alpha(s')} = e^{i\frac{2\pi}{N}} e^{i\alpha(s)}$

- Symmetry group $\boldsymbol{G} = C_N = \{\boldsymbol{e}, \boldsymbol{g}, \ldots, \boldsymbol{g}^{\boldsymbol{N-1}}\}$ $\boldsymbol{g}$: rotation by $2\pi/N$, $\hat{U}(\boldsymbol{g}) = e^{i\frac{2\pi}{N}\hat{L}}$

- Wave functions classifiable according to their transformation properties

$$\psi_{1,2}^{(l)}(\boldsymbol{g}_l^{-\lambda}\boldsymbol{r}) = \tilde{\psi}_{1,2}^{(l)}(\boldsymbol{r}') = e^{i\lambda\frac{2l\pi}{N}}\tilde{\psi}_{1,2}^{(l)}(\boldsymbol{r}) \qquad l=0,1,2,\ldots,N-1$$

- The spinor components transform differently under rotation

- For $\tilde{\psi}_1^{(l)}(\boldsymbol{r})$ $\qquad \tilde{\psi}_2(\boldsymbol{r}') = e^{-i(l-1)\frac{2\pi}{N}}\tilde{\psi}_2(\boldsymbol{r}) \equiv \tilde{\psi}_2^{(l-1)}(\boldsymbol{r}')$

$$\tilde{\psi}_2(s') = ie^{i\alpha(s')}\mathcal{K}^{-1}\tilde{\psi}_1^{(l)}(s') = e^{-i(l-1)\frac{2\pi}{N}}\tilde{\psi}_2(s) \equiv \tilde{\psi}_2^{(l-1)}(s')$$

Entanglement of Symmetry Classes in Equilateral-Triangle NB

BD, Acta Pol. 140, 473 (2021)

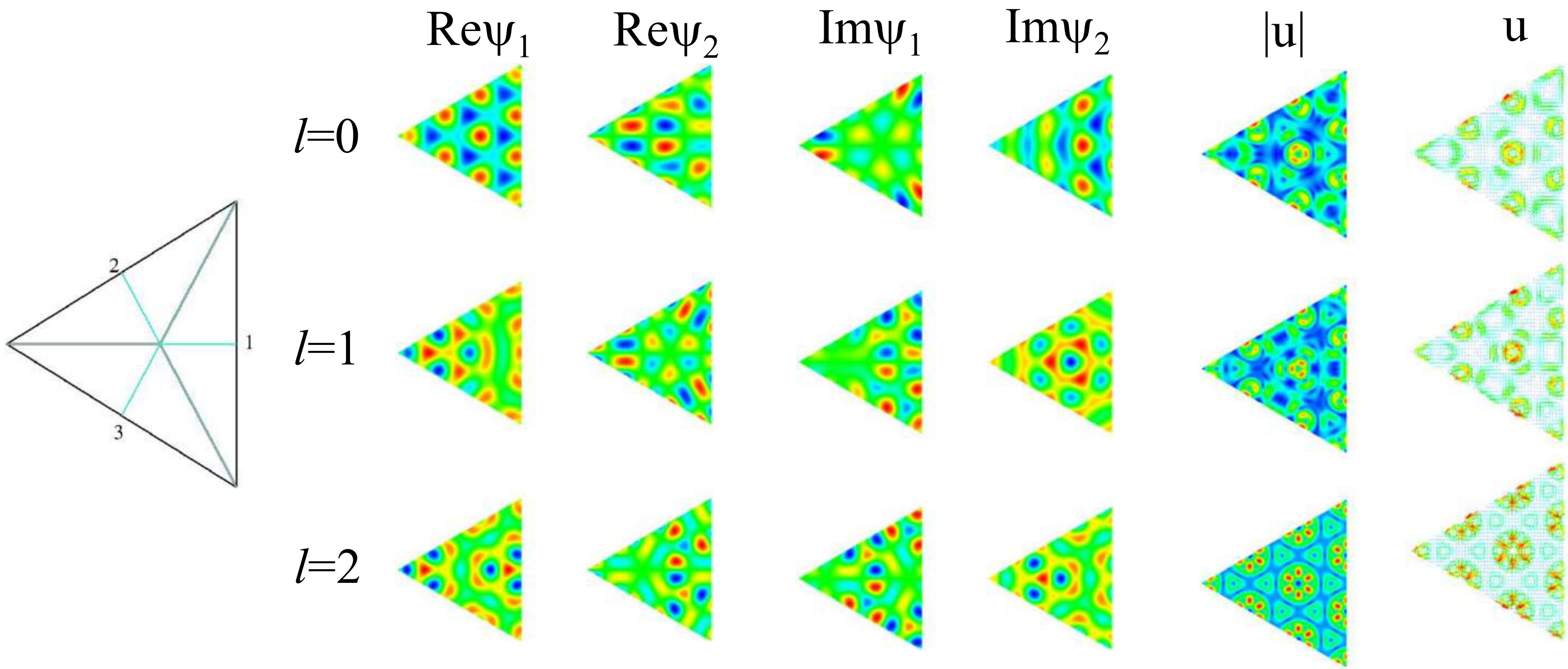

- Symmetry-projected eigenvalue equations with $n=n_1+n_2$, $m=n_1-n_2$

$$\tan\left(\frac{\sqrt{3}}{2}k_x-\tilde{n}\pi\right)= 3\frac{\mathcal{K}\left(\mathcal{K}^2-1\right)\cos\theta_k}{1+\mathcal{K}^4-4\mathcal{K}^2-\mathcal{K}\left(1+\mathcal{K}^2\right)\sin\theta_k+4\mathcal{K}^2\sin^2\theta_k}$$

$$\tan\left(\frac{k_y}{2}-l\frac{2\pi}{3}-\tilde{m}\pi\right) = \sqrt{3}\frac{\frac{\mathcal{K}^2}{2}+\mathcal{K}\sin\theta_k}{1-\frac{\mathcal{K}^2}{2}+\mathcal{K}\sin\theta_k}$$

Symmetry-Projected BIEs for NBs
Zhang & Dietz, PRB 104, 064310 (2021)

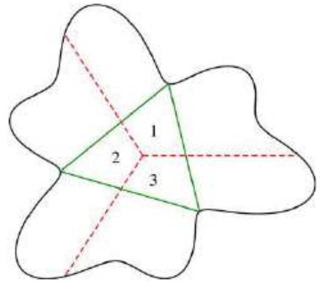

- Boundary-integral equation can be written in the form

$$u(\phi') = \int_0^{2\pi} d\phi |w'(\phi)| Q(k;\phi,\phi') u(\phi) \quad \text{with} \quad u(\phi) = \psi_{1,2}(\phi)$$

- 3fold symmetry implies

$$w\left(\phi + \lambda\frac{2\pi}{3}\right) = e^{i\lambda\frac{2\pi}{3}} w(\phi) \quad \Rightarrow \quad Q\left(k;\phi,\phi' - \lambda\frac{2\pi}{3}\right) = Q\left(k;\phi + \lambda\frac{2\pi}{3},\phi'\right), \phi,\phi' \in [0,\frac{2\pi}{3})$$

- Use 3fold symmetry and define $M_\lambda(k;\phi,\phi') = Q\left(k;\phi + \lambda\frac{2\pi}{3},\phi'\right)$

$$\boldsymbol{u}(\phi') = \int_0^{\frac{2\pi}{3}} d\phi \hat{M}(k;\phi,\phi') \boldsymbol{u}(\phi) \text{ with } \boldsymbol{u}(\phi) = \begin{pmatrix} u_0 \\ u_1 \\ u_2 \end{pmatrix}(\phi) \text{ and } \hat{M}(k;\phi,\phi') = \begin{pmatrix} M_0 & M_1 & M_2 \\ M_2 & M_0 & M_1 \\ M_1 & M_2 & M_0 \end{pmatrix}(k;\phi,\phi')$$

- Symmetry-projected boundary-integral equations

$$u^{(l)}(\phi') = \int_0^{\frac{2\pi}{3}} d\phi \tilde{M}^{(l)}(k;\phi,\phi') u^{(l)}(\phi) \text{ with } \tilde{M}^{(l)}(k;\phi,\phi') = \sum_{\lambda=0}^{2} e^{i\frac{2l\pi}{3}\lambda} M_\lambda(k;\phi,\phi')$$

Wave functions of the Massive Neutrino Billiard with C_3 Symmetry

1500 levels,
$kr_0 \in [0,35]$

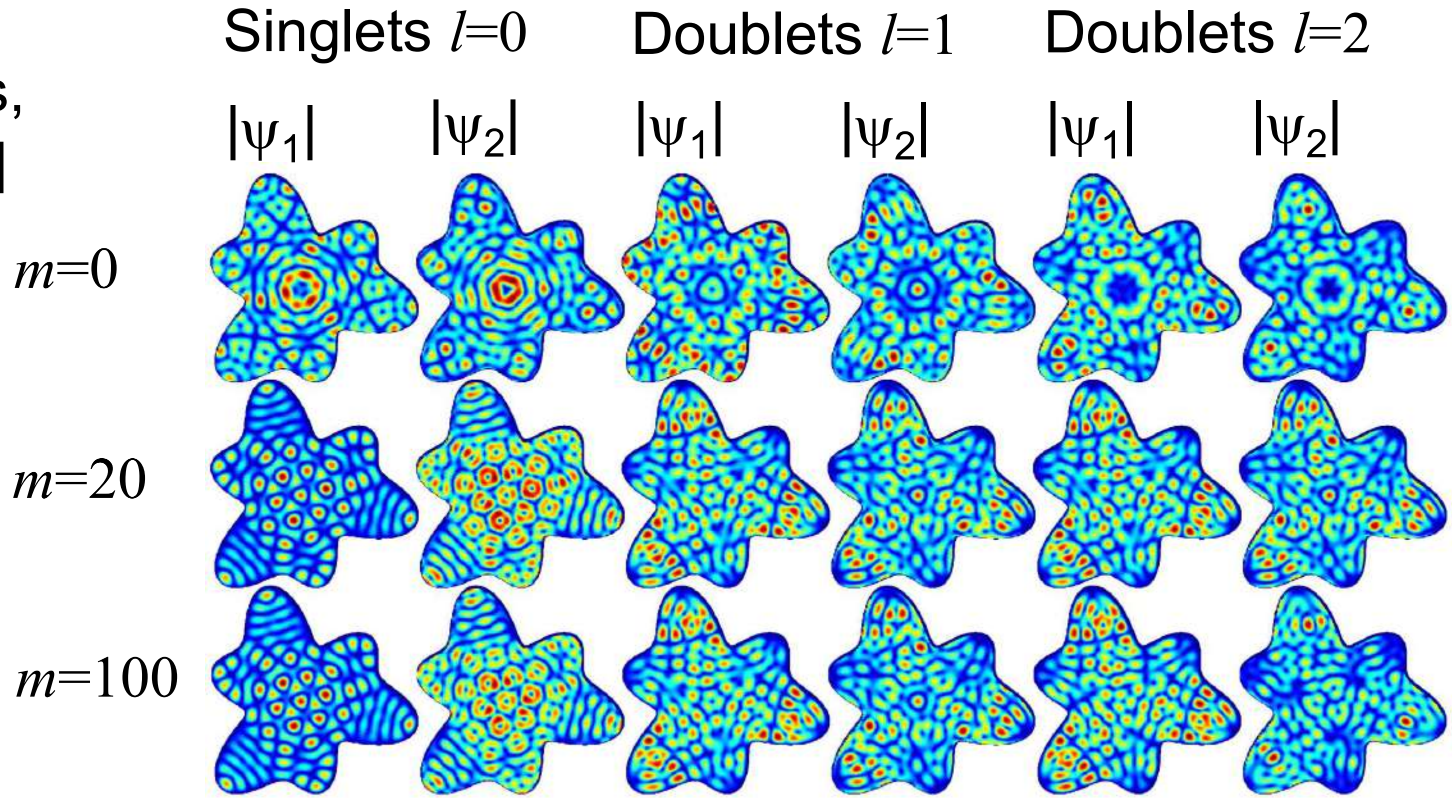

- For $m \to \infty$ the wave function components $\psi_{1,2}$ decouple and $|\psi_2 / \psi_1| \to 0$
- The nodal-line structure of the singlets becomes discernible because $\mathrm{Im}(\psi_{1,2}) \to 0$
- The intensity distributions of the doublets become similar
- The wave functions approach those of the QB

Spectral Properties of Neutrino & Quantum Billiards

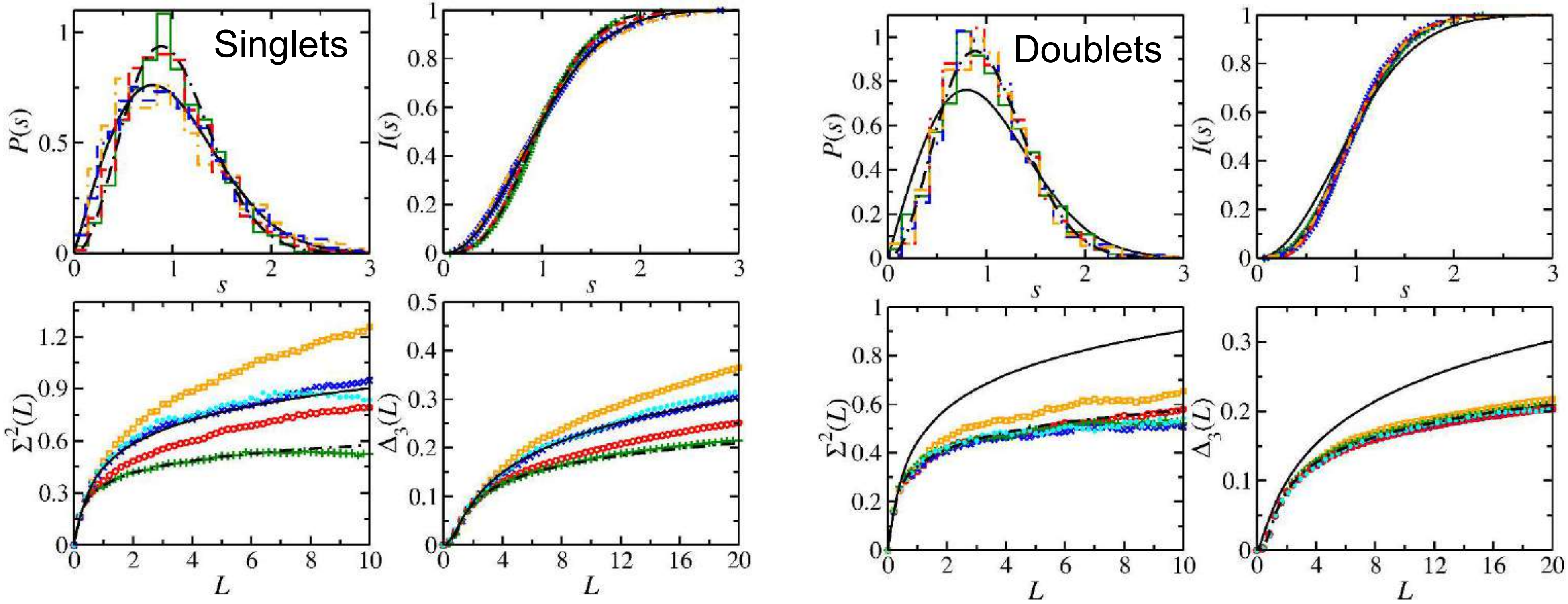

- Spectral properties for mass m=0, m=50, m=100 (100), and for the QB
- Non-generic orbits manifest themselves as slow oscillations in $N^{fluc}(k)$
- Spectral properties are close to GUE for m=0 and to that of the QB for m≥100

Lengths Spectra of Neutrino Billiards

All eigenvalues (l=0,1,2)

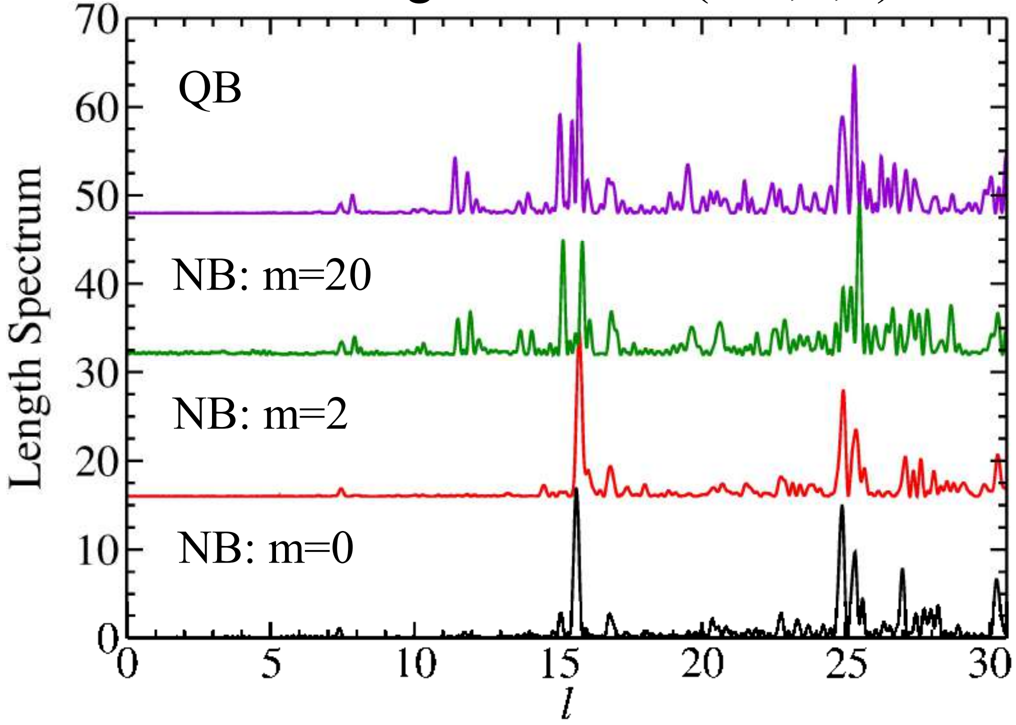

Singlets l=0

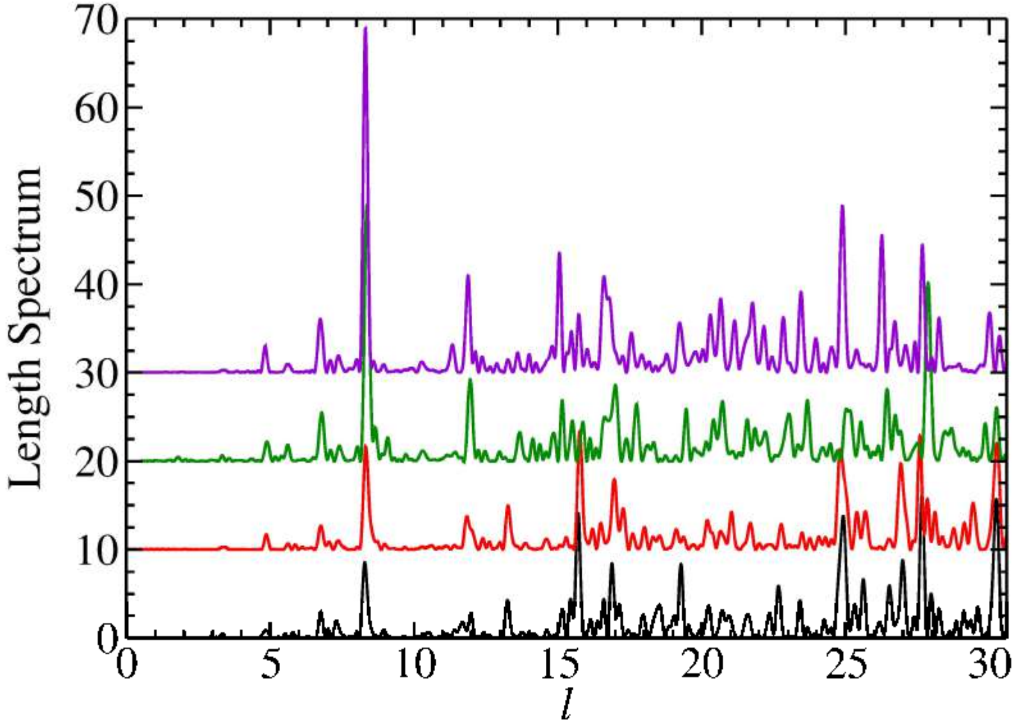

- For m=0 POs with an odd number of reflections are missing
- For m=20 the length spectrum exhibits peaks at the lengths of all POs
- For the singlets some peaks disappear with increasing m

$\Rightarrow$ pseudo orbits

Lengths Spectra of the Doublets of Neutrino Billiard

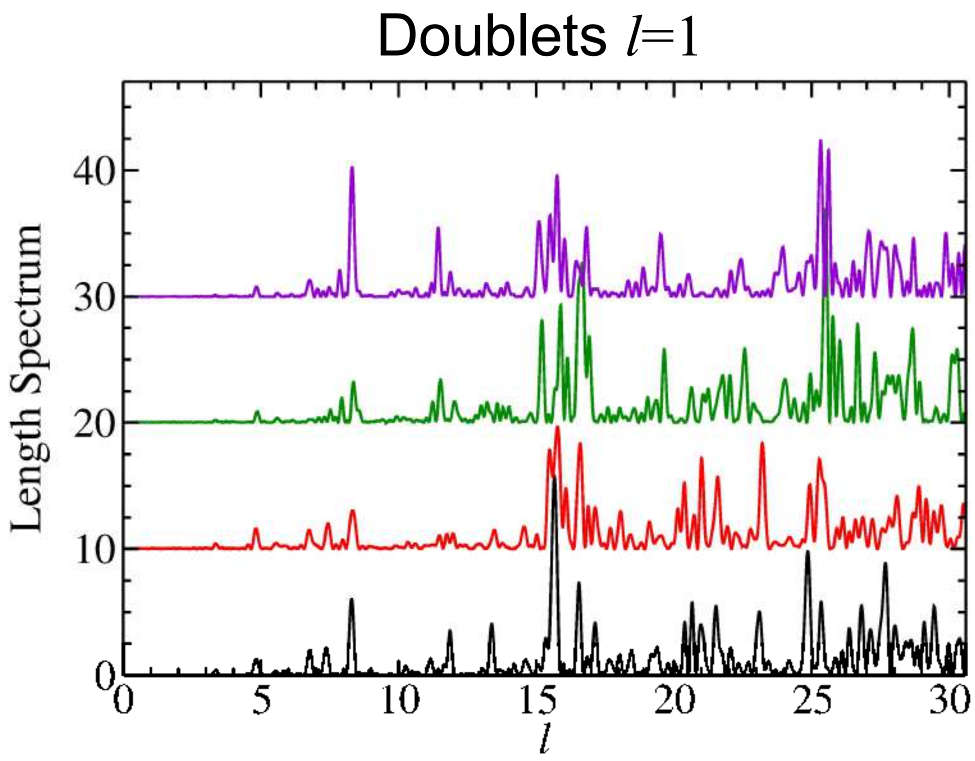

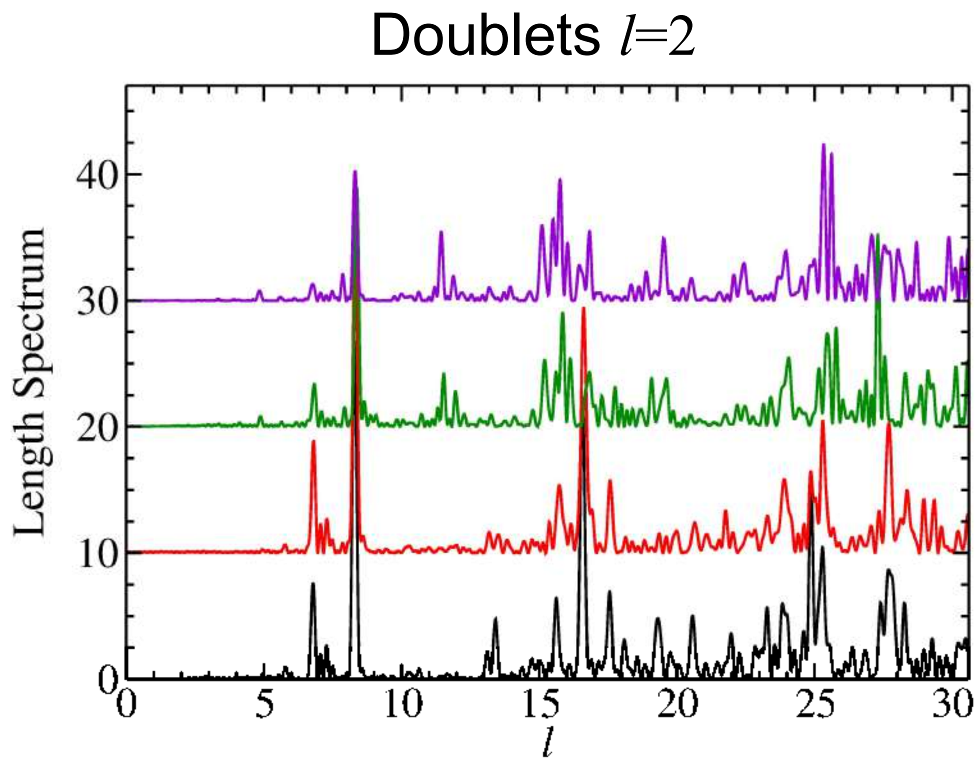

- The lengths spectra differ for small m and become similar for $m \approx 100$
- The occurrence of peaks / interference of POs depends on m and the direction of propagation of the POs and thus on l

$\rightarrow$ The doublets exhibit peaks at the lengths of different pseudo orbits

Momentum Distributions, Wave Functions & Currents of a Square NB (l=1)

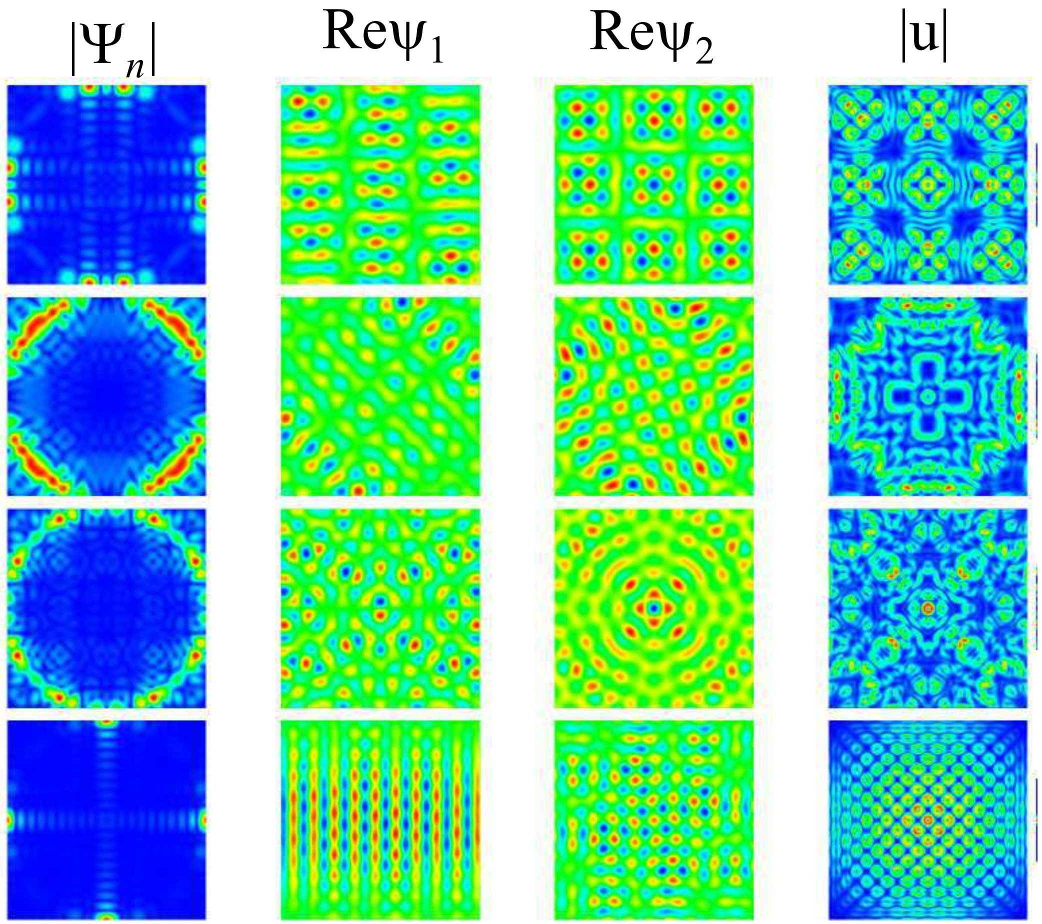

Local current:

$$\hat{\boldsymbol{u}} = \boldsymbol{\nabla}_{\boldsymbol{p}} \hat{H}_D = c\hat{\boldsymbol{\sigma}}, \ \boldsymbol{u}(\boldsymbol{r}) = c\psi^{\dagger}\hat{\boldsymbol{\sigma}}\psi$$

Momentum distribution:

$$\tilde{\psi}_n(q_x, q_y) = \iint_{\Omega} dx dy \psi_n(x, y) e^{-i\boldsymbol{q}\boldsymbol{r}}$$

- The square has a fourfold symmetry ⇒ the spinor components can be classified according to their transformation properties under rotation by $\pi/2$

Spectral Properties of Square NBs

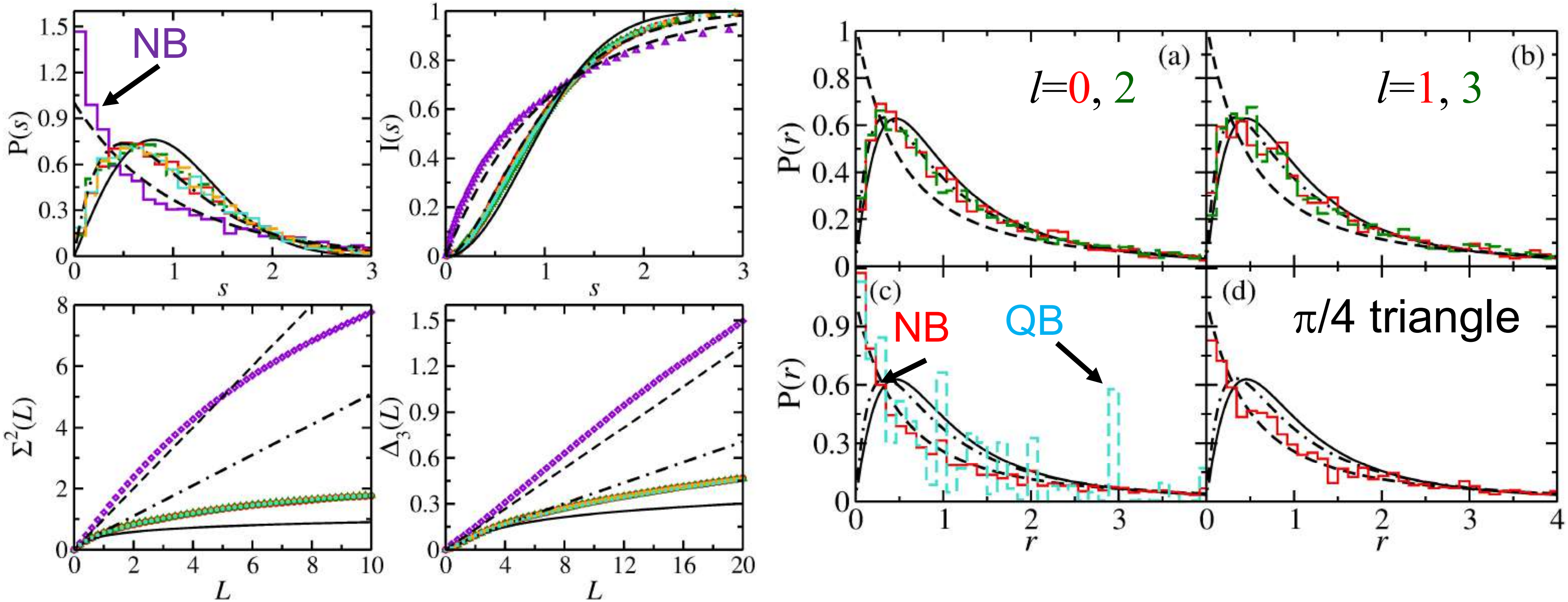

- The square QB is an untypical system with integrable dynamics
- The spectral properties of the square NB agree with Poisson

→ overshootings are due to accidental degeneracies

- The spectral properties of the symmetry-projected eigenstates with $l=0$, $l=1$, $l=2$, $l=3$ are close to Semi-Poisson

Length Spectrum of massless Square NB

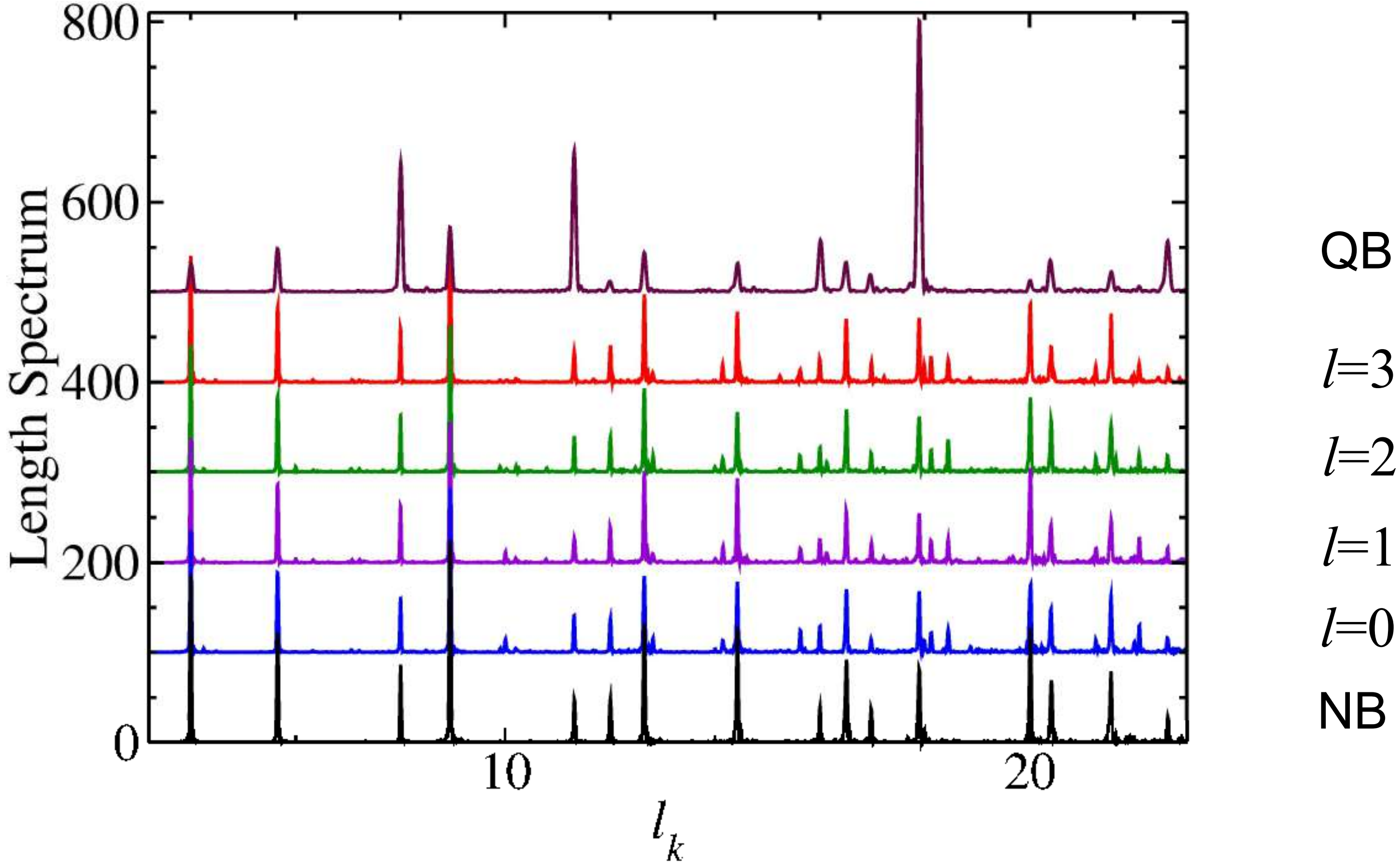

- Generally, the length spectra of the NBs exhibit peaks only at lengths of POs with an even number of reflections at the boundary
- For the symmetry-projected cases peaks appear at lengths of pseudo orbits

Wave Functions and Currents of Rectangular NB

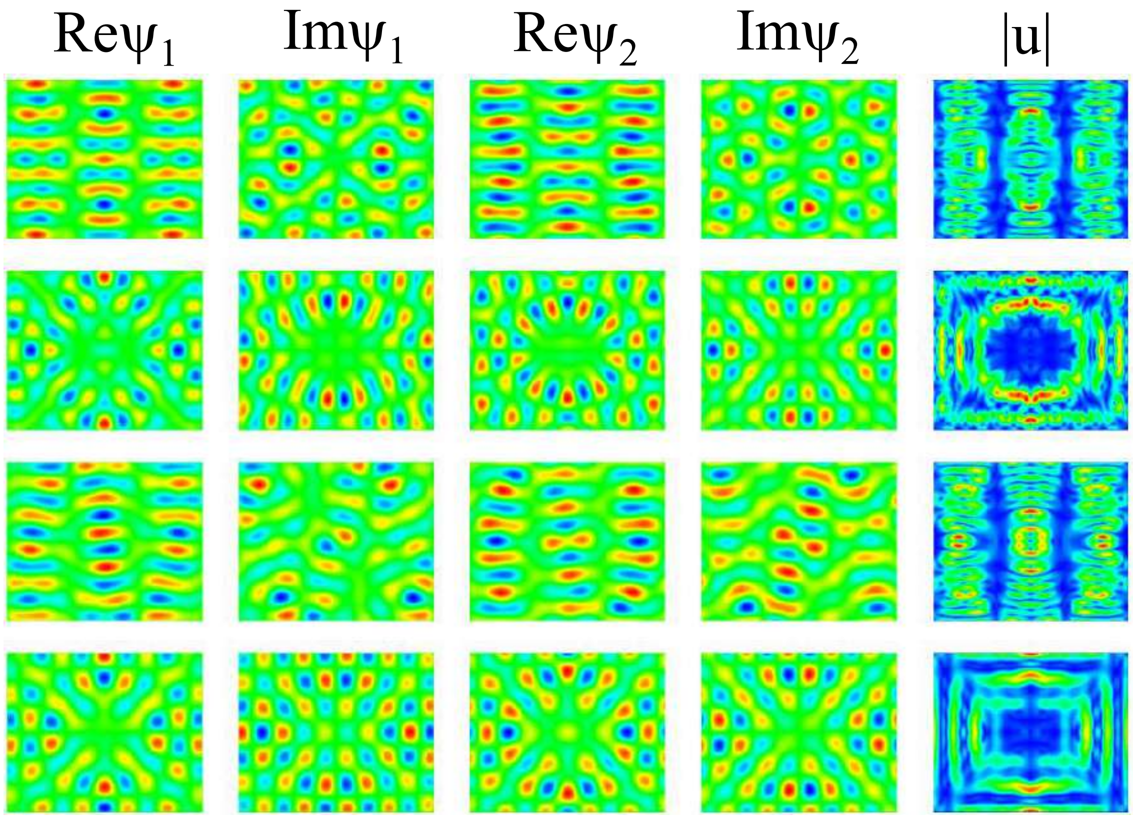

Local current:

$$\hat{\boldsymbol{u}} = \boldsymbol{\nabla}_{\boldsymbol{p}} \hat{H}_D = c\hat{\boldsymbol{\sigma}},\ \boldsymbol{u}(\boldsymbol{r}) = c\psi^{\dagger}\hat{\boldsymbol{\sigma}}\psi$$

- The rectangle has a reflection symmetry with respect to the x- and y-axis $\Rightarrow$ it has a twofold symmetry
- All spinor components are either symmetric or antisymmetric with respect to rotation by π

Ratio distributions of the Rectangular QB & NB

All eigenstates

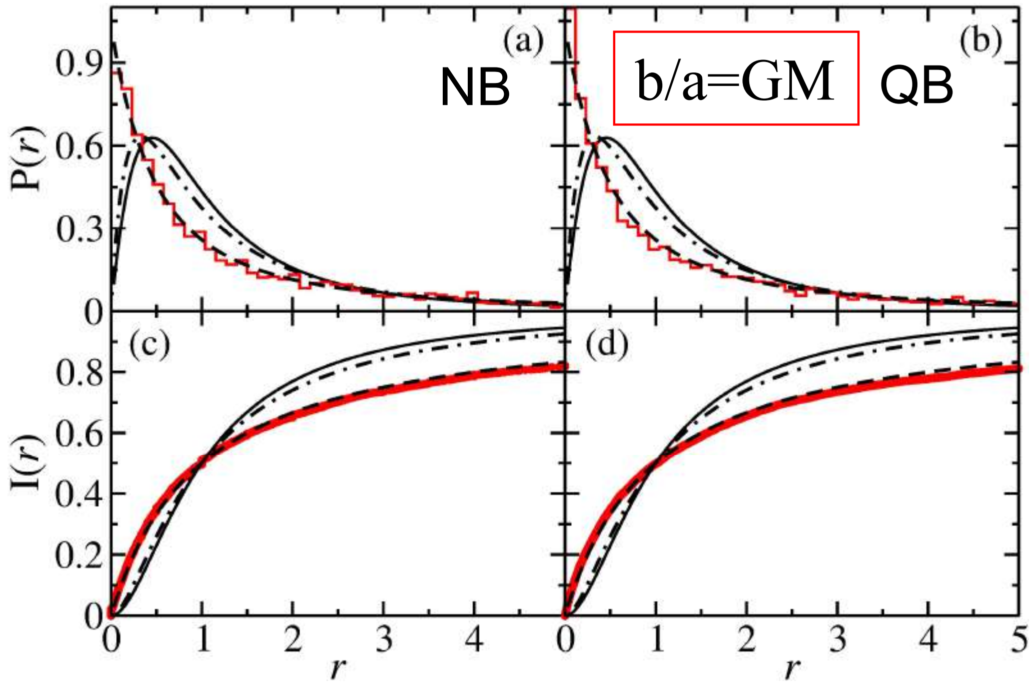

Symmetry-projected eigenstates of the NB

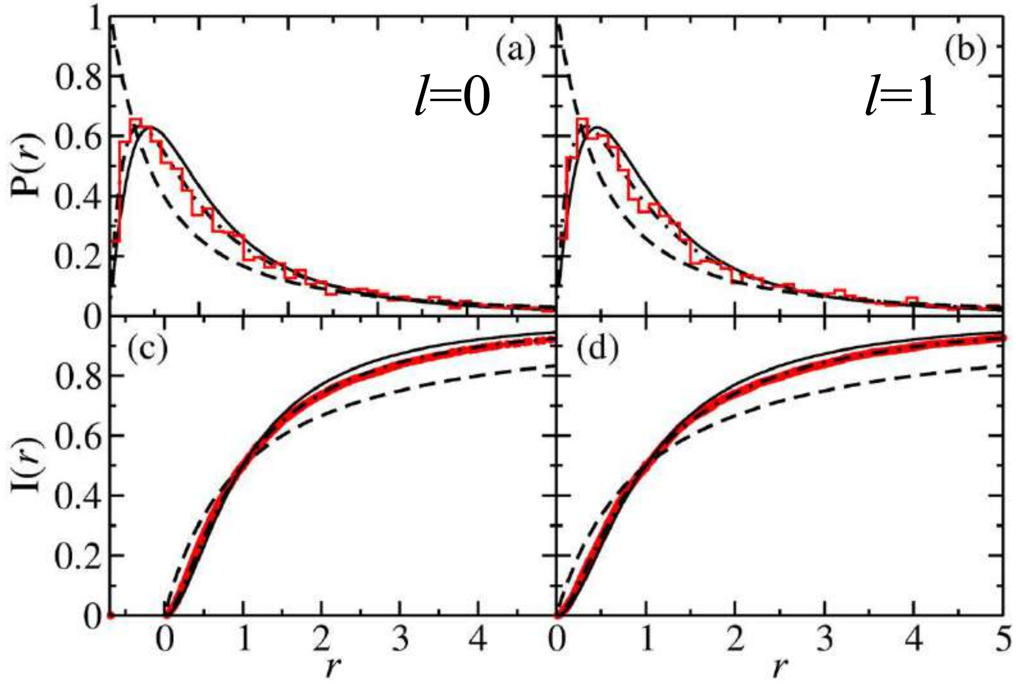

- The spectral properties of the symmetry-projected eigenstates with $l=0$ and $l=1$ are close to Semi-Poisson for all ratios of a/b
- How do the spectral properties change when destroying the N-fold symmetry by cutting the NB along symmetry lines?

Momentum Distributions, Wave Functions & Currents of a Triangle NB

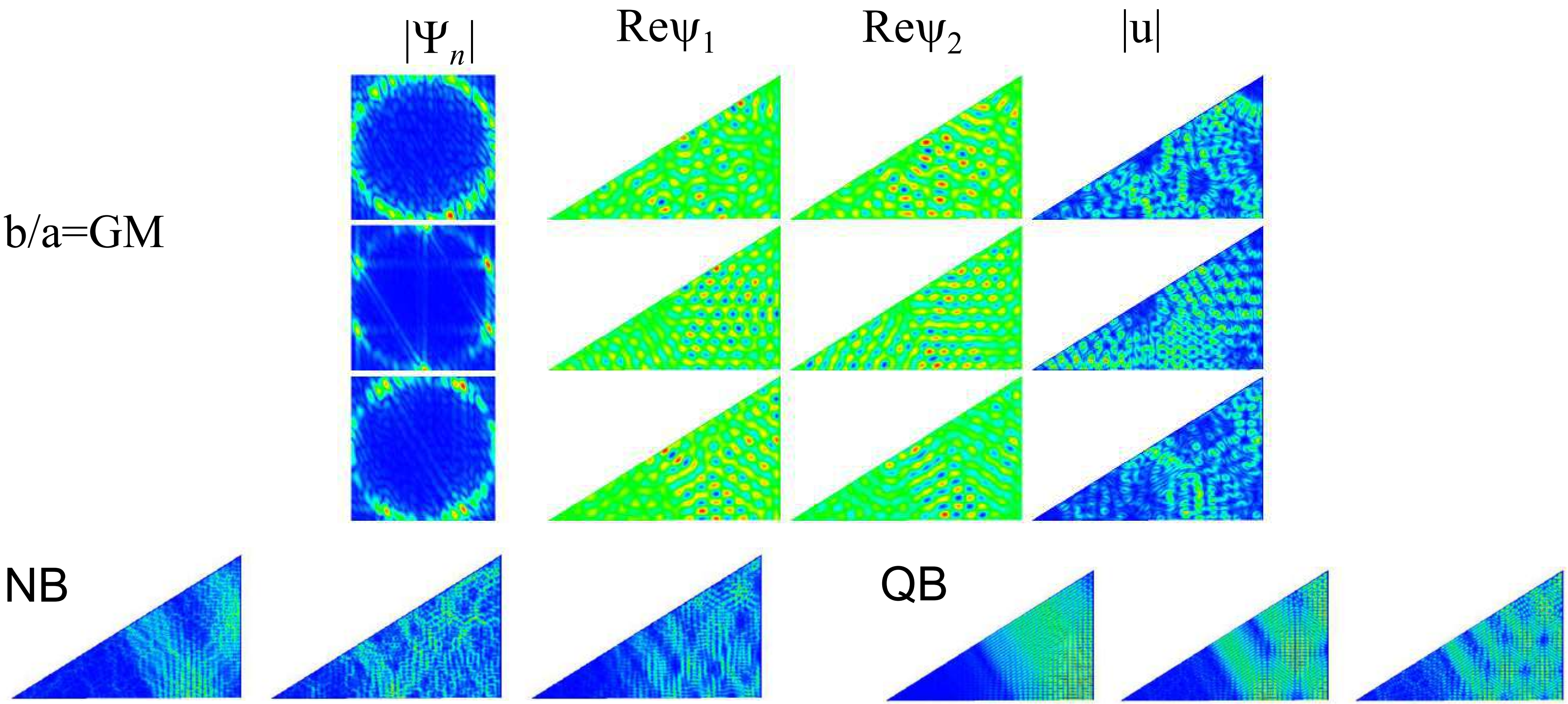

- Triangular billiards are obtained by cutting the rectangular billiards long the diagonal $\rightarrow$ symmetry-reduced
- The NB and QB exhibit similar scarred wave functions

Some Characteristics of Right-Triangle QBs

- Rectangular and right-triangle billiards with inner angles $\alpha=\pi/n$ are integrable and exhibit untypical spectral properties
- Right-triangle billiards with inner angles $\alpha=\pi m/n$ ($m\neq 1$, n,m incommensurable) are pseudointegrable

$\Rightarrow$ Exhibit intermediate statistics, i.e., levels repel each other and the nearest-neighbor spacing distribution decays exponentially

- Right-triangle with irrational α/π may exhibit GOE-like behavior
- We found quarter-Poisson for NBs with b/a irrational if it is semi-Poisson for the corresponding QBs
- Atas et al., JPA **46**, 355204 (2013):

$$P_\nu(s) = \frac{\Gamma(\nu+2)^{\nu+1}}{\Gamma(\nu+1)^{\nu+2}} s^\nu \exp\left(-\frac{\Gamma(\nu+2)}{\Gamma(\nu+1)} s\right) \quad \mathcal{P}_\nu(r) = \frac{\Gamma(2\nu+2)\Gamma^2(\nu+2)}{(\nu+1)^2\Gamma^4(\nu+1)} \frac{r^\nu}{(1+r)^{2\nu+2}}$$

- Semi-Poisson: delete every second number from a Poisson sequence
- Quarter-Poisson: delete every second number from a semi-Poisson sequence

Spectral Properties of Triangular NBs with b/a=GM and b/a=2

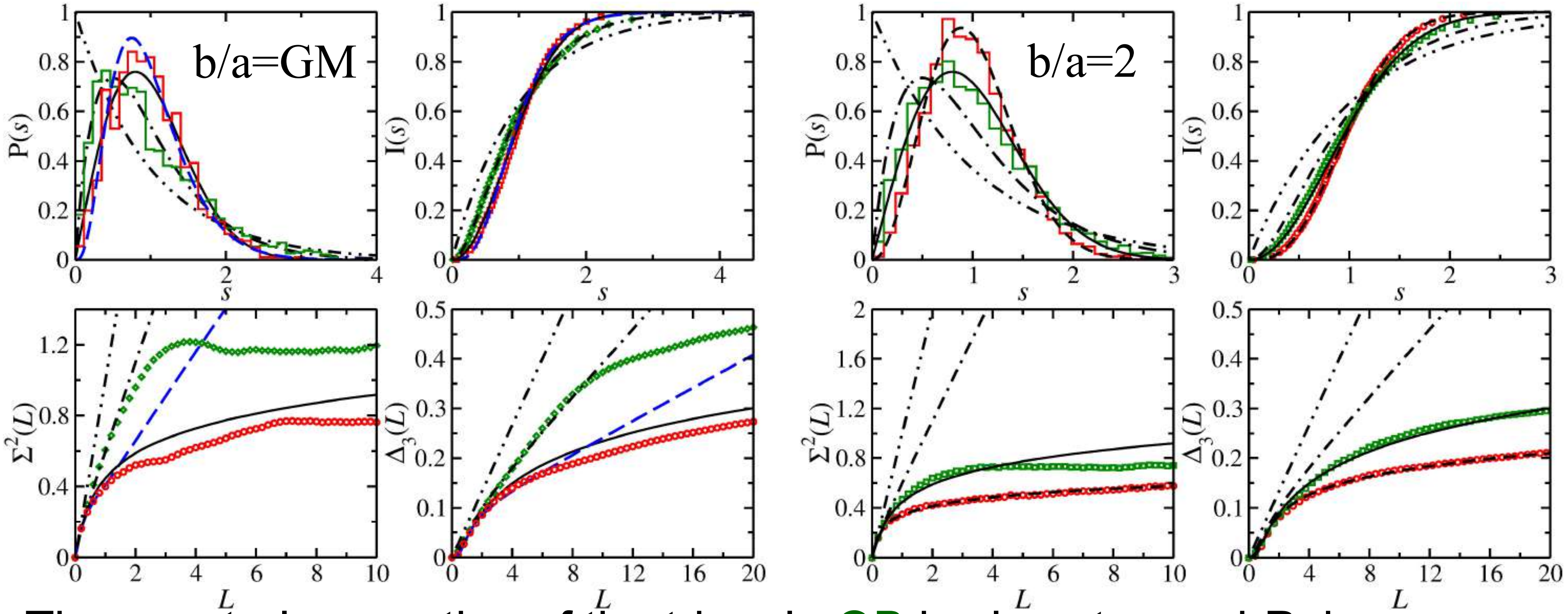

- The spectral properties of the triangle QB is close to semi-Poisson statistics → linear level repulsion
- The spectral properties of the triangle NB is close to quarter-Poisson statistics → cubic level repulsion
- For b/a=2 the QB / NB shows GOE / GUE. Deviations are due to scarred functions

Circle Sector QB

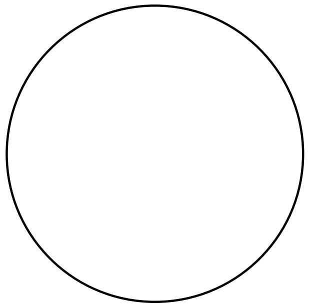

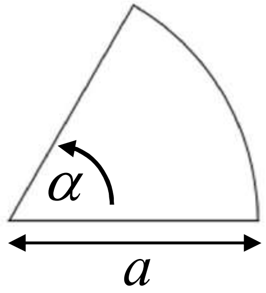

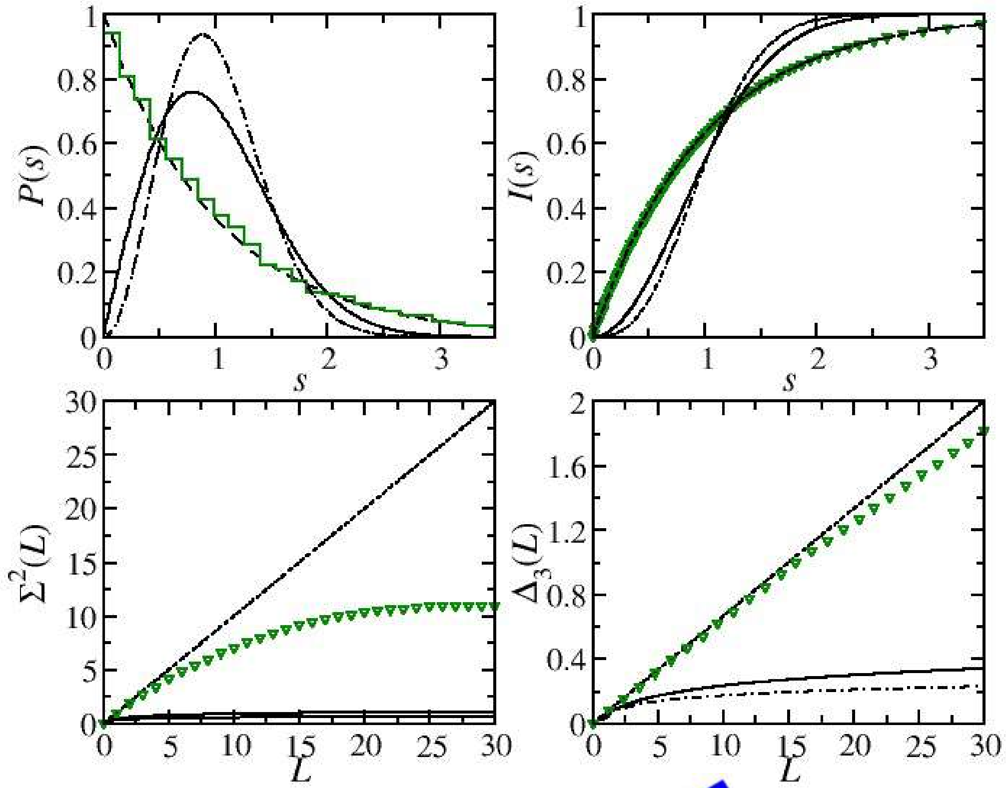

$$\Omega = \left\{ (r,\varphi) \; : \; 0 < r < a, \; |\varphi| < \frac{\alpha}{2} \right\}$$

- Eigenvalues:

$$J_{\frac{\pi \ell}{\alpha}}(k_{\ell,n} a) = 0$$

- Eigenfunctions:

$$\psi_{\ell,n}(r,\varphi) = \sin\left[\frac{\pi \ell}{\alpha} \left(\varphi + \frac{\alpha}{2} \right) \right] J_{\frac{\pi \ell}{\alpha}}(k_{\ell,n} r)$$

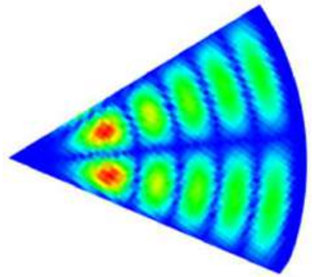

15° Circle Sector @ Lower Band Edge

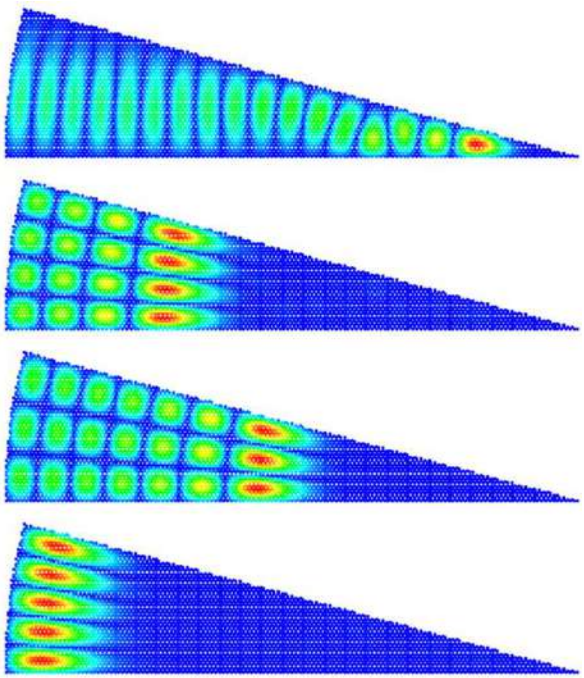

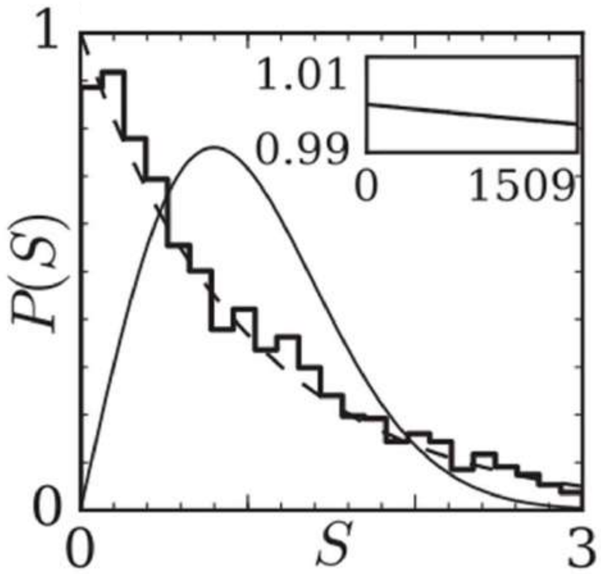

- At the band edges the spectral properties coincide with those of the corresponding quantum billiard for any shape
- The system is effectively described by the Schrödinger equation

15° Circle Sector: Below the VHS

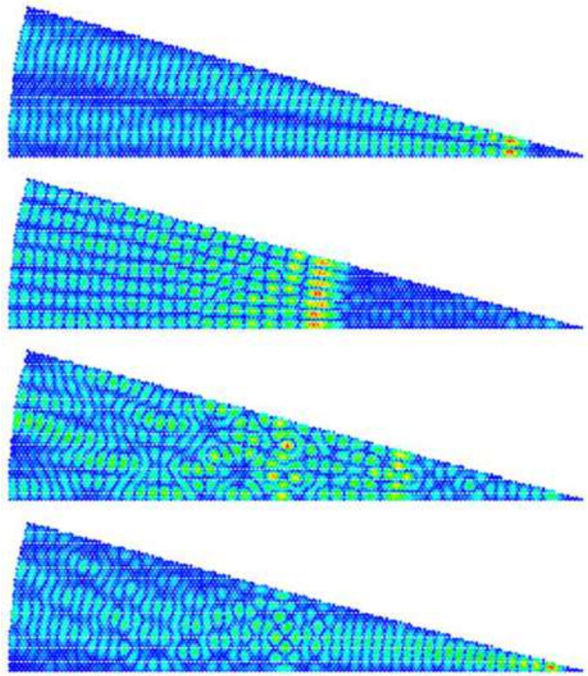

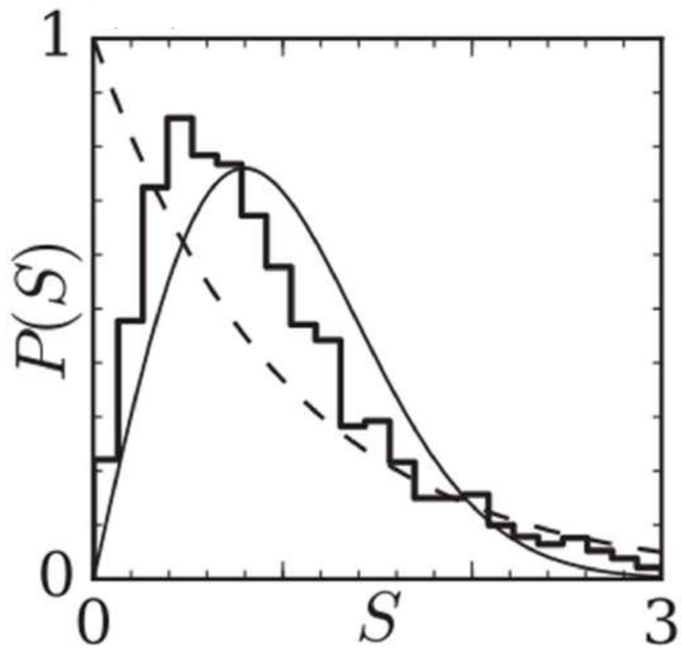

- The spectral properties are intermediate between Poisson and GOE
- With increasing energy the lattice structure starts to prevail leading to the occurrence of the van Hove singularities in the spectral density and the Dirac point

15° Circle Sector @ Dirac Point

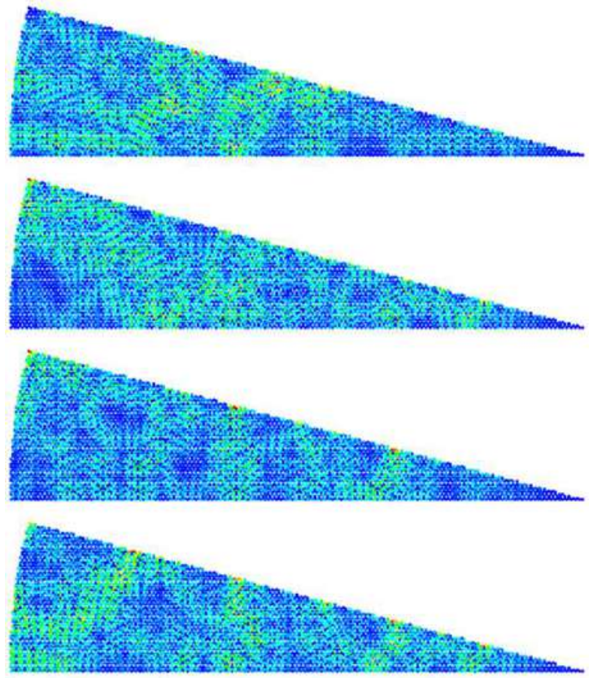

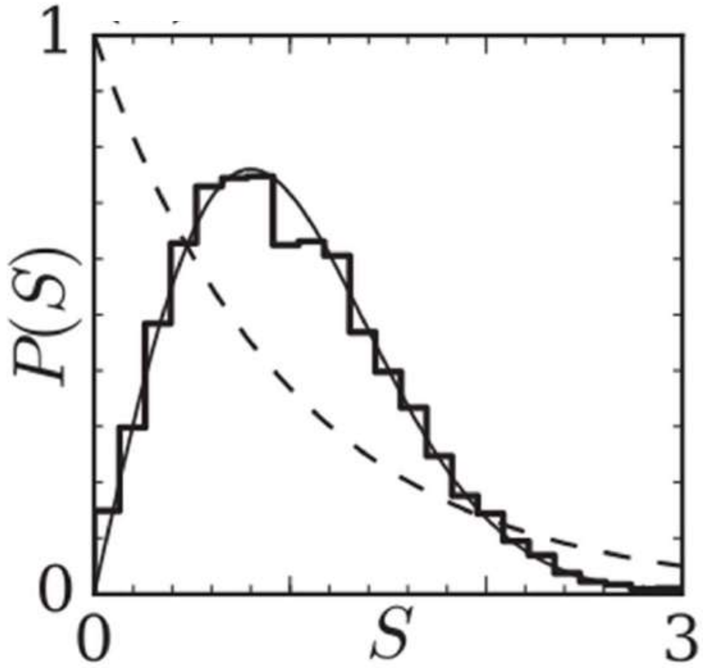

- Near the Dirac points the spectral properties coincide with those of chaotic systems with preserved time-reversal invariance (GOE)
- Attributed to the edge structure implying different boundary conditions for the independent triangular lattices

→ Spectral properties of relativistic quantum billiards ?

Spectral Properties of the 3fold-Symmetric Solutions of the Circle NB and the 120° Circle Sector NB

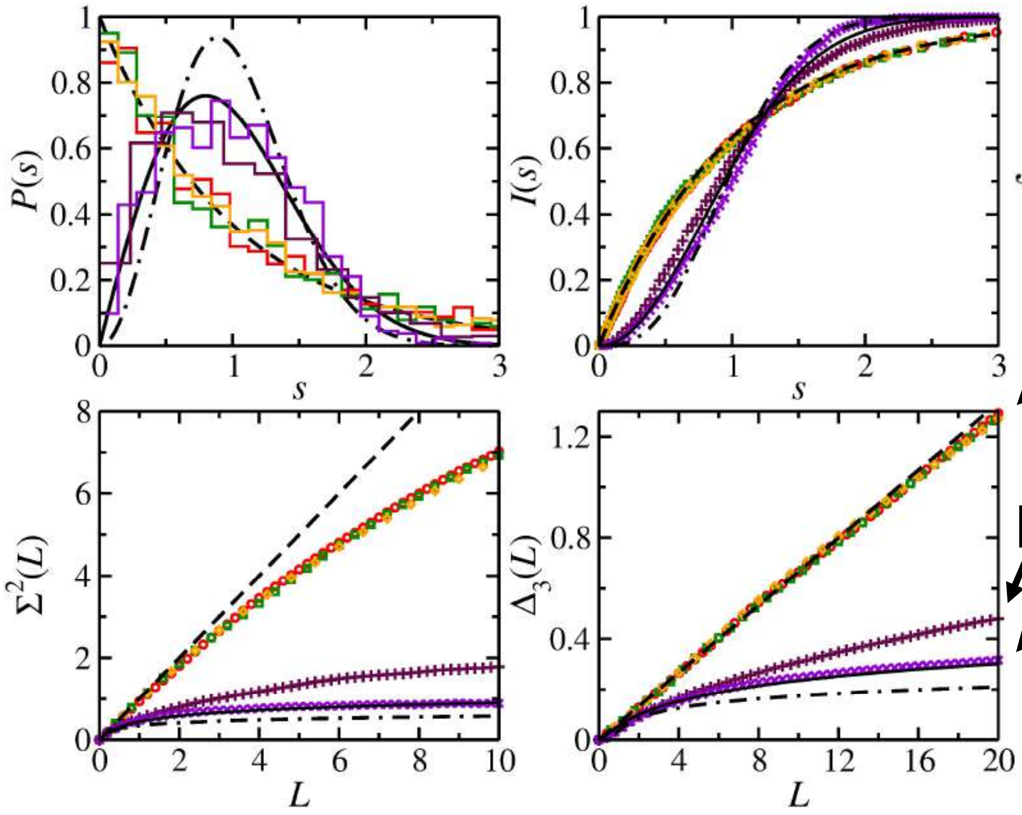

$$J_{3m+\lambda}(k\mathcal{R}) = \mathcal{K} J_{3m+\lambda+1}(k\mathcal{R}).\ \lambda = 0, 1, 2$$

NB

NB after extracting contributions of the diameter orbit by employing its trace formula

- Circle neutrino billiard:

$$\psi_1^{nl} = J_l(k_n r) e^{il\phi}, \psi_2^{nl} = iJ_{l+1}(k_n r) e^{i(l+1)\phi}$$

$$J_m(k\mathcal{R}) = \mathcal{K} J_{m+1}(k\mathcal{R}).$$

- Trace formula for diameter orbit:

$$\rho^{diam}(k;\tilde{\beta}) = \sqrt{\frac{k\mathcal{R}}{\pi}} \sum_{p\,\mathrm{even}} \frac{\cos\left(2kp\mathcal{R} - p\theta_\beta + \frac{\pi}{4}\right)}{\sqrt{p}}.$$

Spectral Properties of Massive Half-Circle NB

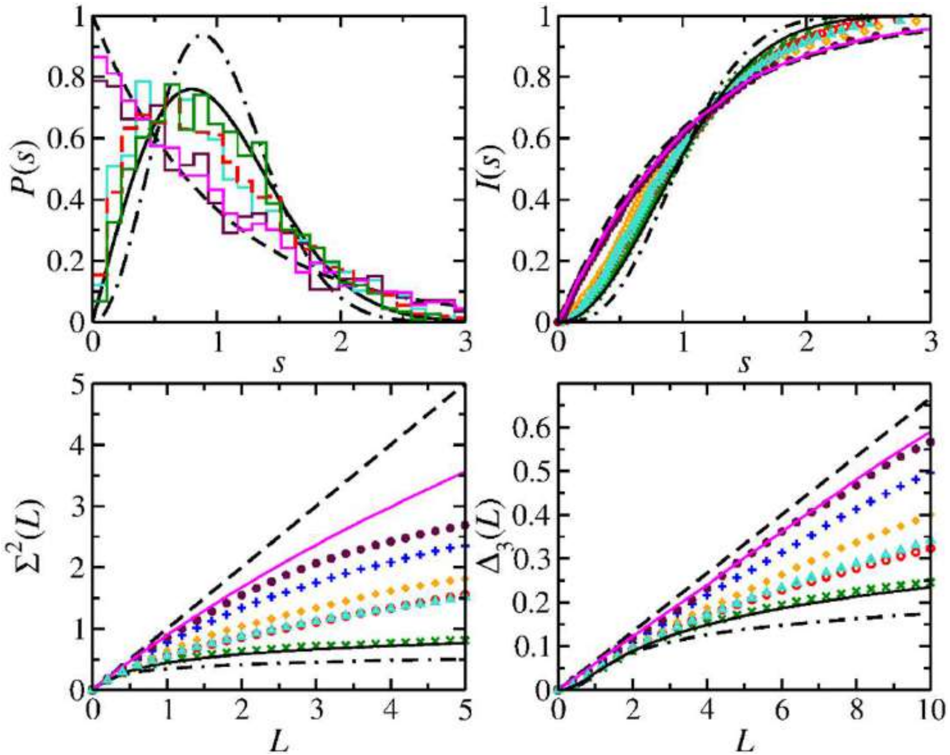

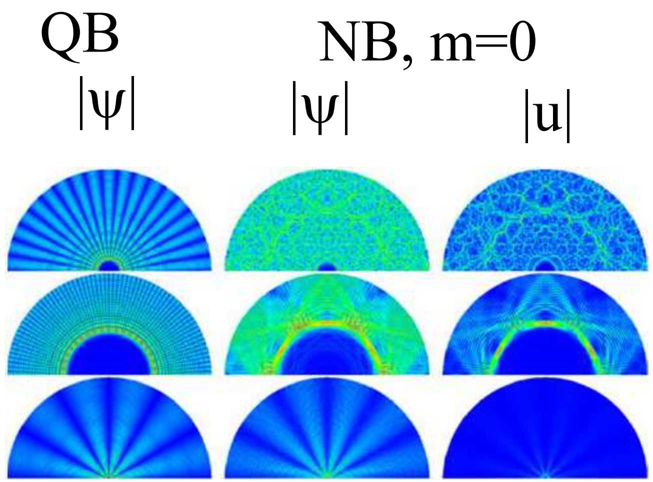

- Spectral properties for mass m=0 (0), 10, 20, 50, 100, and for the QB
- Contributions of diameter orbit are extracted by employing its trace formula
- Deviations from Poisson due to intermingling of symmetry classes of the spinor components and discontinuity in the BCs at the corners
- NBs do not have a classical counterpart → Semiclassical limit?

Semiclassical Approach: Length Spectra & Quantum Poincaré Section Map

- Length spectrum $|\tilde{\rho}(l)| = |\int_0^{k_{max}} \mathrm{d}k e^{ikl} \rho_{fluc}(k)|$
- Semiclassical approach: semiclassical approximation for the fluctuating part of spectral density in terms of a sum over periodic orbits
- Husimi function on PSOS: Projection of boundary function onto a coherent state on the billiard boundary
- Husimi functions: $$\mathrm{H}_j(s,p) = \frac{1}{2\pi k_j} \frac{1}{\int_0^{\mathcal{L}} ds' \left|\partial_{n'}\psi(s')\right|^2} \left| \int_0^{\mathcal{L}} ds' \partial_{n'}\psi(s') C^{\delta}_{(s',p)}(s';k_j) \right|^2$$
- Coherent state: $$C^{\delta}_{(s,p)}(s';k_j) = \left(\frac{k_j}{\pi\delta^2}\right)^{1/4} \sum_{m=-\infty}^{\infty} \exp\left(ipk_j\left(s'-s+m\mathcal{L}\right) - \frac{k_j}{2\delta^2}\left(s'-s+m\mathcal{L}\right)^2\right)$$
- Definition of Birkhoff coordinates
- The Poincaré map is defined in terms of the arclength s_n and the momentum $p_n = |\mathbf{p}| \sin\theta_n$ at n th bounce with the boundary

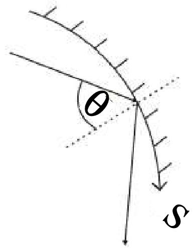

Trace Formula for the Spectral Density of Massive Neutrino Billiards

BD & Z. Li, PRE102, 042214 (2020)

- Quantization condition deduced from the BIEs for Massive NBs

$$\boldsymbol{u}(s') = \hat{\boldsymbol{Q}}(k)\boldsymbol{u}(s) \quad \Rightarrow \quad \det\left(\mathbb{1} - \hat{\boldsymbol{Q}}(k)\right) = 0 \quad \Rightarrow \quad \rho^{fluc}(k) = \frac{1}{\pi}\Im\sum_{p=1}^{\infty}\frac{1}{p}\frac{\mathrm{d}}{\mathrm{d}k}\left[\mathrm{Tr}\left(\hat{\boldsymbol{Q}}\right)^p(k)\right]$$

- Trace formula is a sum over the periodic orbits of the classical billiard

$$\Im\frac{1}{p}\frac{\mathrm{d}}{\mathrm{d}k}\left[\mathrm{Tr}\left(\hat{\boldsymbol{Q}}\right)^p(k)\right] = \Re\sum_{\gamma_p}\cos\left(\Phi_{\gamma_p} - p\frac{\pi}{2}\right)\mathcal{B}^{\tilde{\beta}}_{\gamma_p}e^{i\Gamma^{\tilde{\beta}}_{\gamma_p}}\mathcal{A}_{\gamma_p}e^{i\Theta_{\gamma_p}} + \Re\sum_{\gamma_p}\cos\left(\Phi_{\gamma_p} + p\frac{\pi}{2}\right)\tilde{\mathcal{B}}^{\tilde{\beta}}_{\gamma_p}e^{i\tilde{\Gamma}^{\tilde{\beta}}_{\gamma_p}}\mathcal{A}_{\gamma_p}e^{i\Theta_{\gamma_p}}$$

QB

$$\mathcal{A}_{\gamma_p} = \frac{l^{(p)}_{\mathrm{PO}}}{r_{\mathrm{PO}}\sqrt{|\mathrm{Tr}M^{(p)}_{\mathrm{PO}} - 2|}}$$

$$\Theta_{\gamma_p} = kl^{(p)}_{\mathrm{PO}} - \frac{\pi}{2}\mu^{(p)}_{\mathrm{PO}},$$

Gutzwiller

- The factor $\mathcal{B}^{(l)\tilde{\beta}}_{\gamma_p}e^{i\Gamma^{(l)}_{\gamma_p}}$ depends on m and the direction of propagation of the PO

$$\rho^{fluc}(k;\tilde{\beta}) \xrightarrow{\tilde{\beta}\to\infty} \frac{1}{\pi}\Re\sum_{\gamma_p}\mathcal{A}_{\gamma_p}e^{i\Theta_{\gamma_p}}$$

$$\rho^{fluc}(k;\tilde{\beta}) \xrightarrow{\tilde{\beta}\to 0} \frac{1}{\pi}\Re\sum_{\gamma_p}(-1)^p\cos\left(\Phi_{\gamma_p}\right)\cos\left(p\frac{\pi}{2}\right)\mathcal{A}_{\gamma_p}e^{i\Theta_{\gamma_p}} \quad \Rightarrow$$

Only POs with even # reflections p contribute

Length Spectra of 1/2-Circle and 1/4-Ellipse NBs

Half circle

m=0

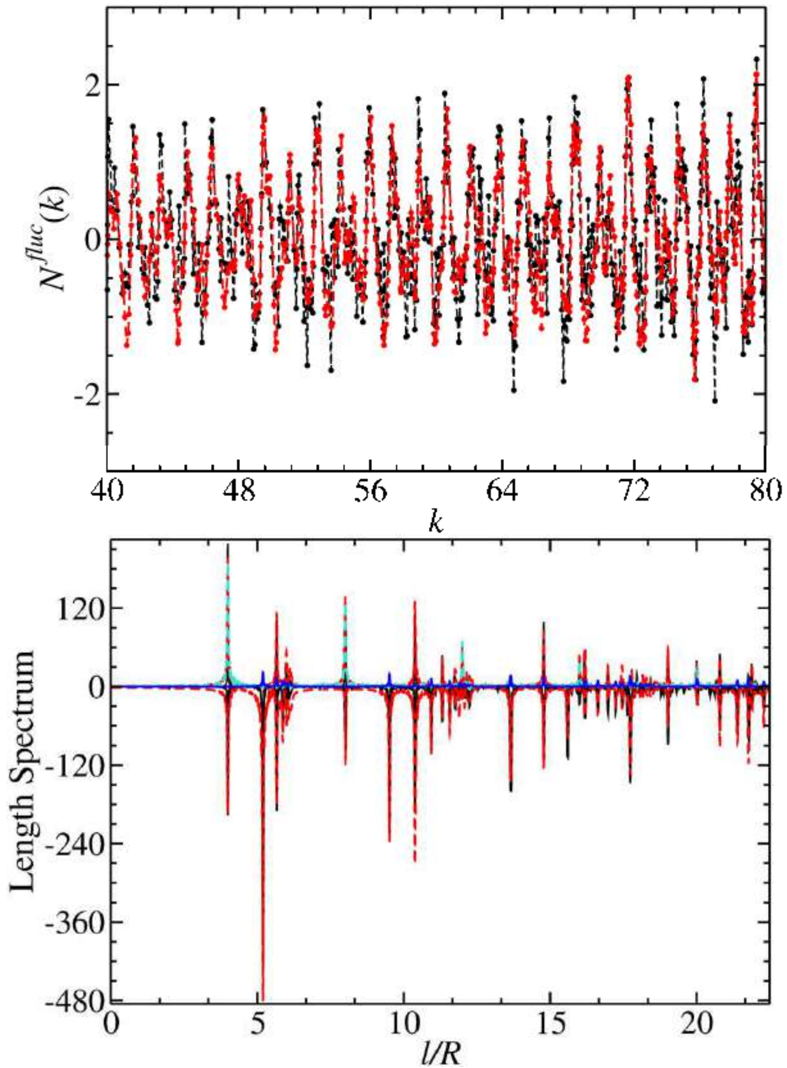

Quarter ellipse

m=0

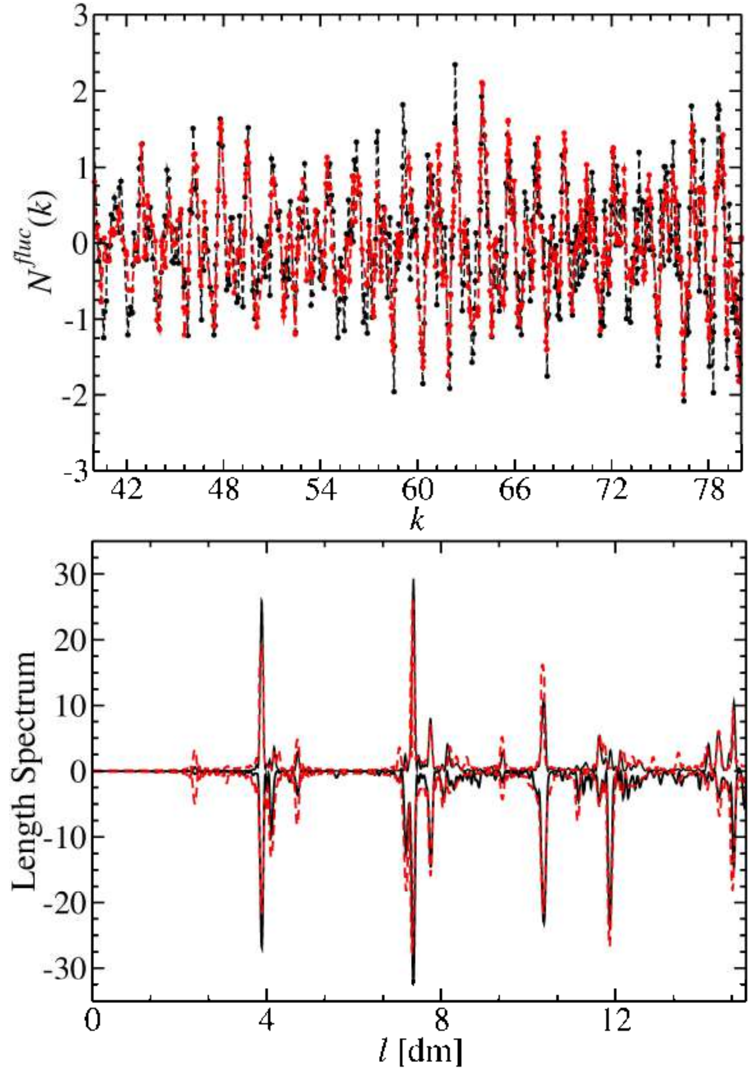

- The length spectra of the NBs exhibit peaks only at length of POs

Husimi Distribution of the First Wave Function Component of 1/2-Circle NB

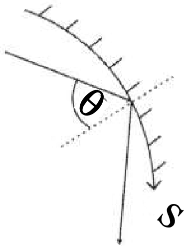

p = sin θ

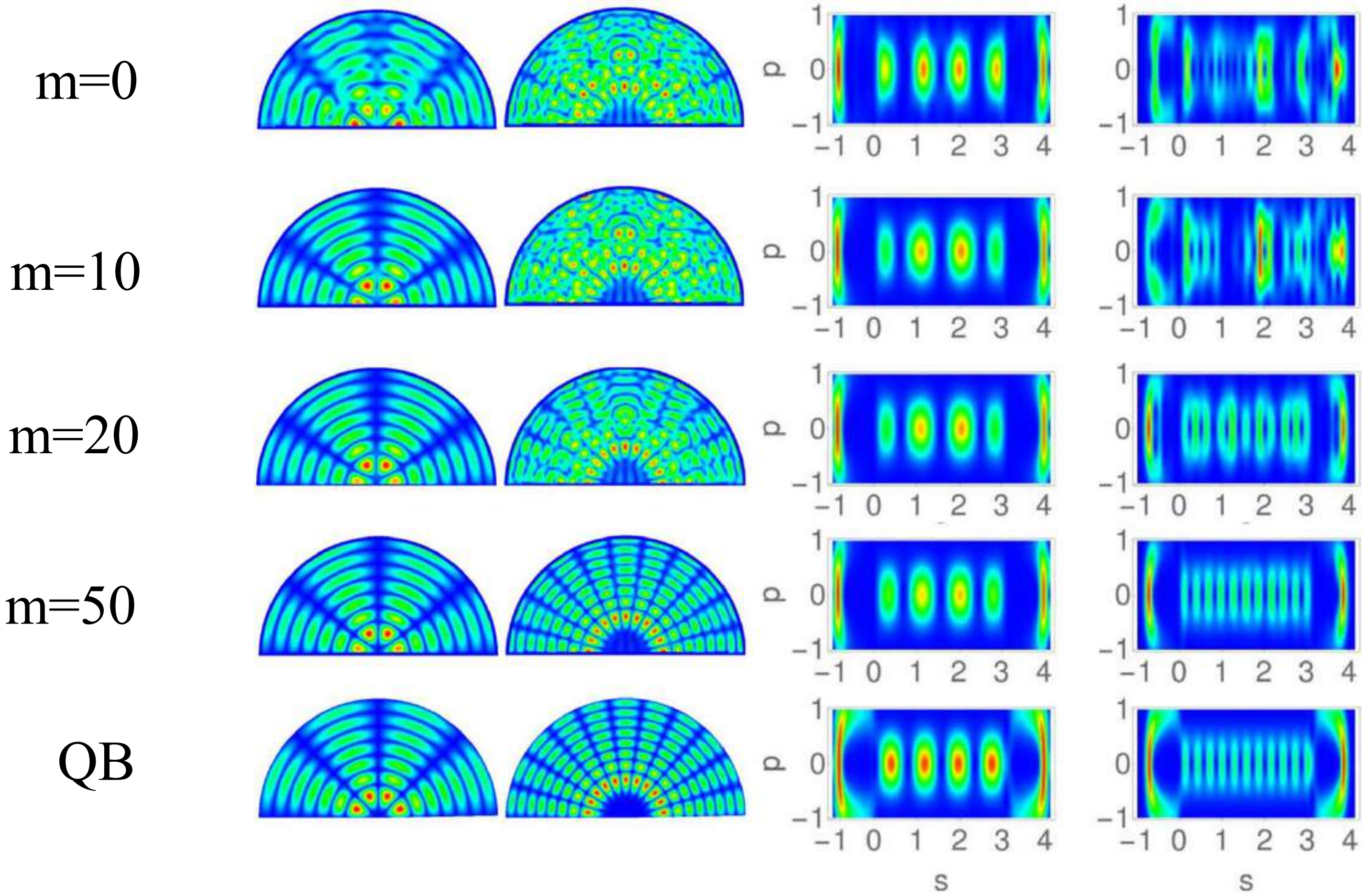

- For m≈50 the Husimi distribution is close to that of the QB, for smaller mass it is similar to it for diameter-orbit like WFs

Spectral Properties of Massive 1/4-Ellipse NB

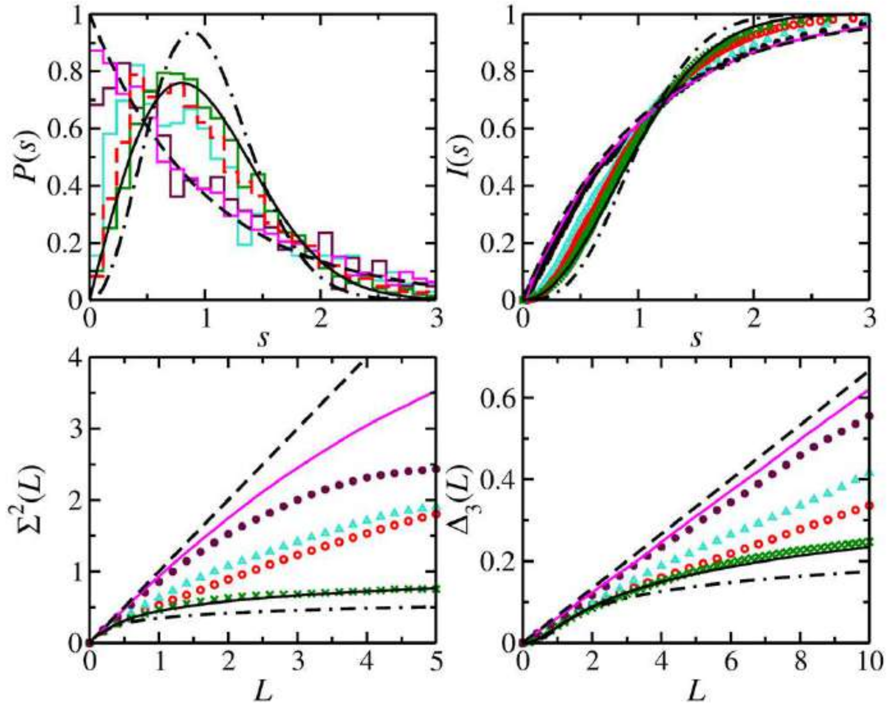

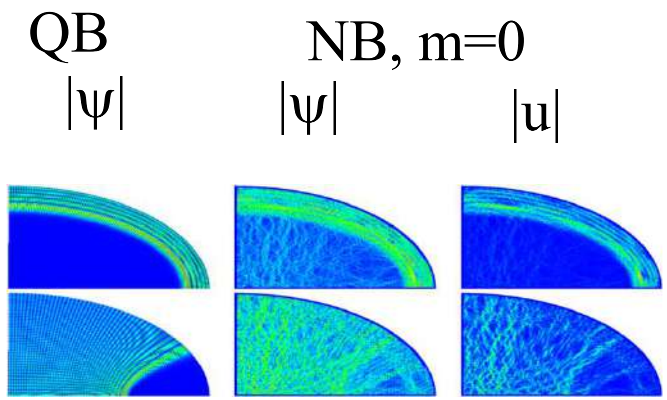

- Spectral properties for mass m=0 (0), 10, 20, 50, 100, and for the QB
- Contributions of diameter orbit are extracted by employing its trace formula
- Deviations from Poisson due to intermingling of symmetry classes of the spinor components and discontinuity in the BCs at the corners

Husimi Distribution of the First Wave Function Component of Quarter-Ellipse NB

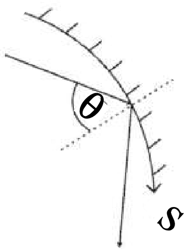

$p = \sin\theta$

m=0

m=10

m=20

m=50

QB

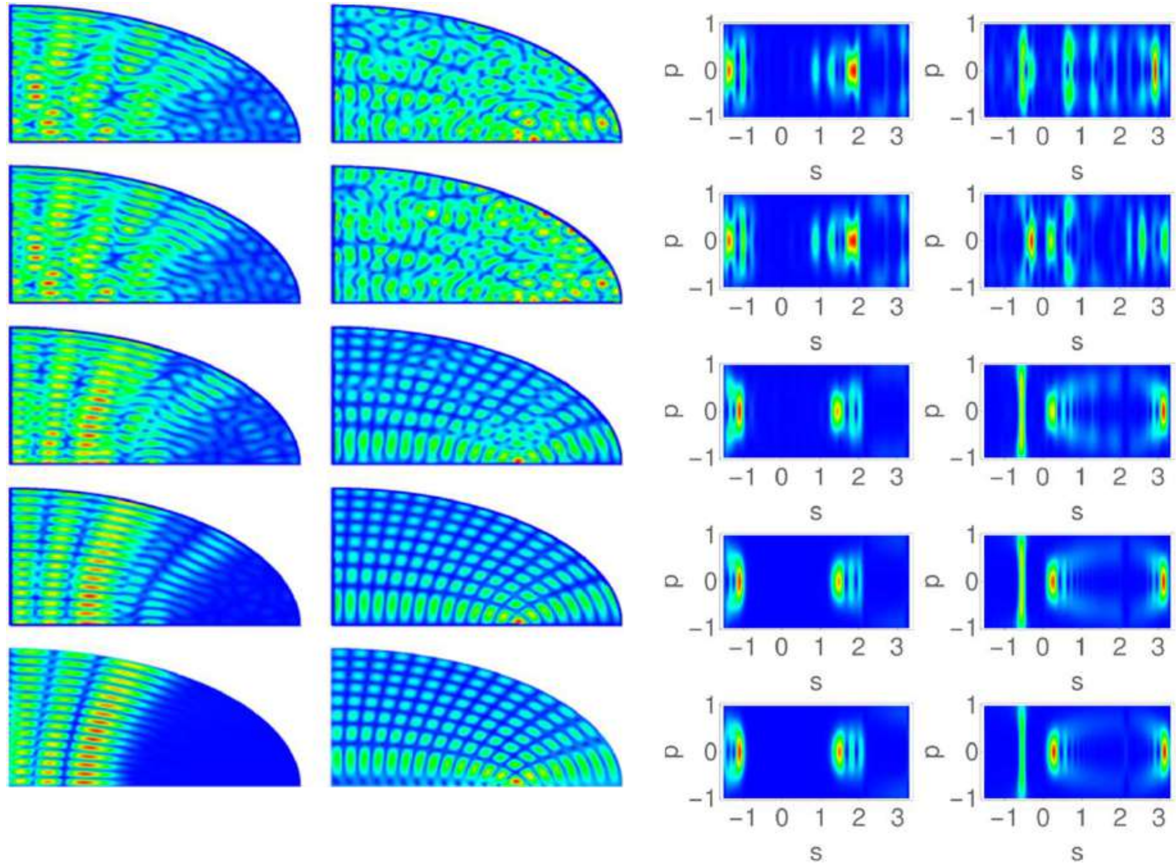

- For m≈20 the Husimi distribution is close to that of the QB, for smaller mass it is similar to it for diameter-orbit like WFs

Constant Width Billiards

O. Knill, Elemente der Mathemarik 53, 89 (1998)

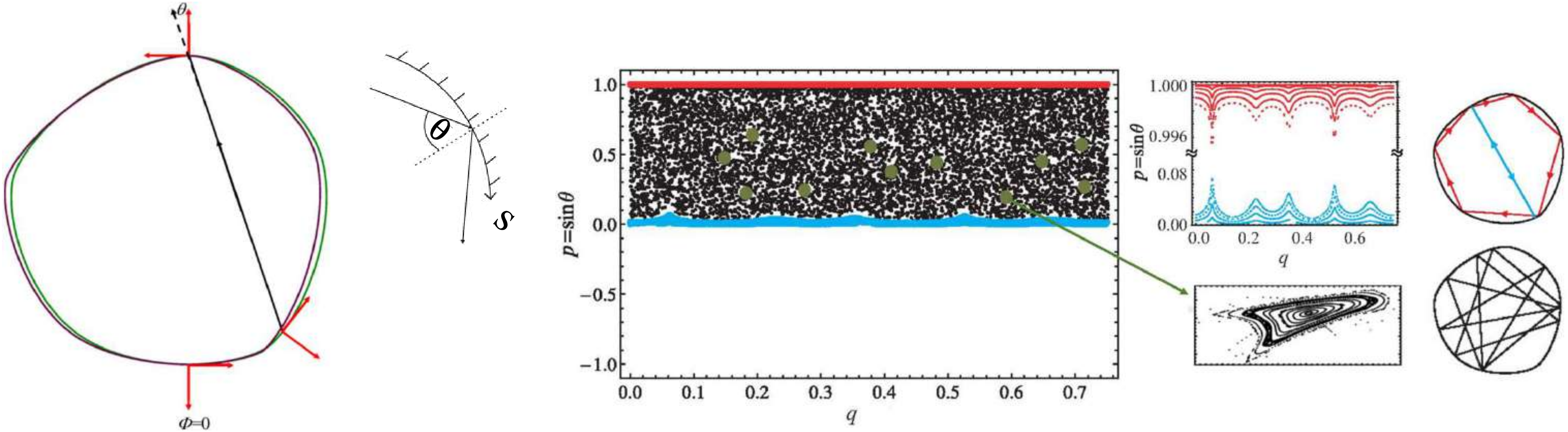

- Classical dynamics is unidirectional
- Change from clockwise to anti-clockwise motion classically forbidden
- In quantum billiard transition from p>0 to p<0 possible due to tunneling

$$w(\phi) = -R_0 i e^{i\phi} - i a_3 \left[\frac{(e^{i4\phi} - 1)}{4} + \frac{(e^{-i2\phi} - 1)}{2} \right] - i a_5 \left[\frac{(e^{i6\phi} - 1)}{6} - \frac{(e^{-i4\phi} - 1)}{4} \right], \; \phi \in [0, 2\pi)$$

$$w'(\phi) = \mathcal{R}(\phi) e^{i\phi}, \; \mathcal{R}(\phi) = R_0 + 2 i a_3 \sin(3\phi) + 2 a_5 \cos(5\phi), \; \mathcal{R}(\phi) = \mathcal{R}^*(\phi)$$

$$\boldsymbol{t}(\phi) = [\cos\phi, \sin\phi] \qquad \boldsymbol{n}(\phi) = \left[\cos\left(\phi - \frac{\pi}{2}\right), \sin\left(\phi - \frac{\pi}{2}\right)\right]$$

Spectra of the CW NB & QB

- The spectra of the QB & NB can be separated into singlets and nearly-degenerate doublets
- Singlets correspond to diameter orbit $(p=0)$ of circle NB & QB
- For the QB dynamical tunneling leads to a splitting of the degenerate eigenvalues of the circle billiard into doublets of nearly degenerate ones
- Doublets can be separated into two independent sequences
- The circle NB has no degeneracies
- For the NB the spectra can be separated into eigenstates corresponding to Husimi functions localized in the upper or lower part of the PSOS

Comparison of Wave Functions & Husimi Functions of the QB and Massless NB

QB

NB

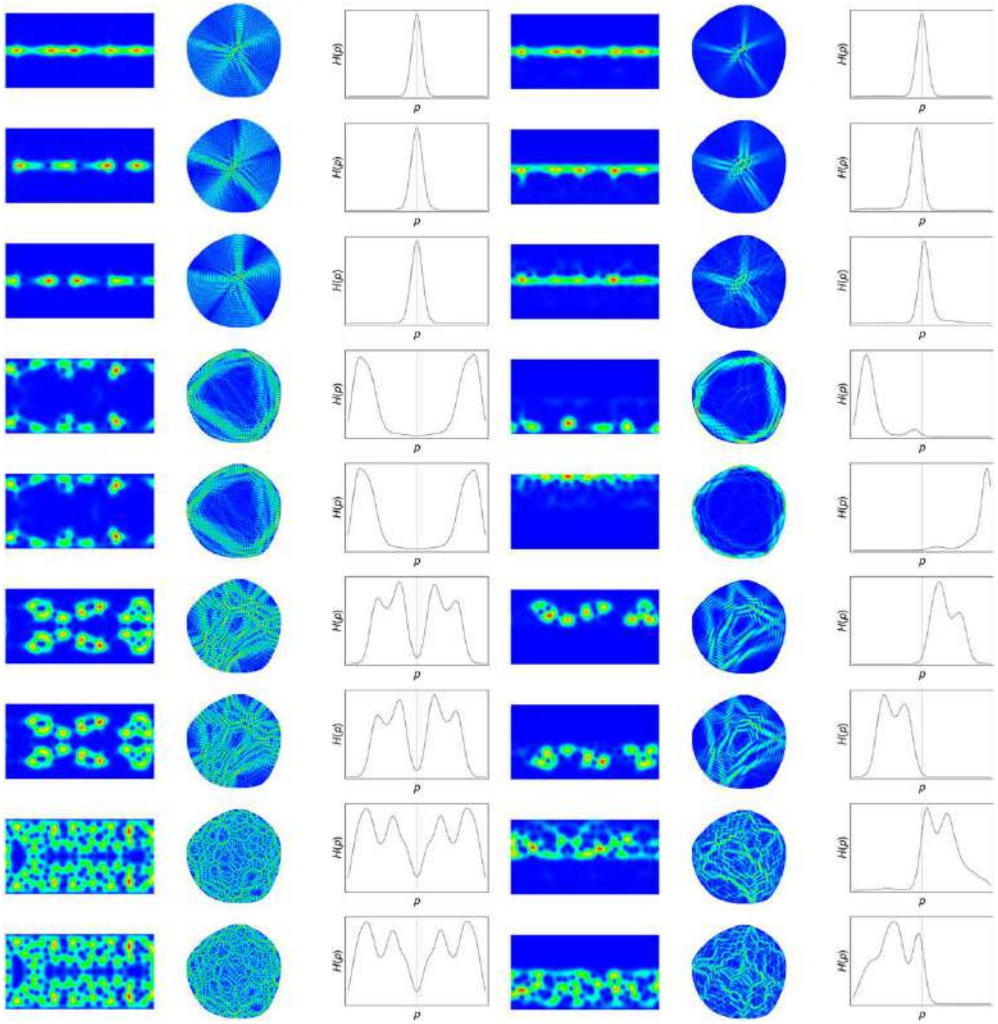

adjacent eigenvalues (nearly degenerate doublets)

eigenvalues separated by $\approx$ 4 others

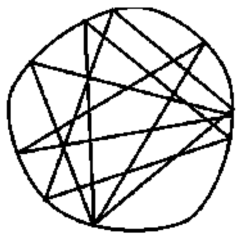

located on small islands!

- NB: $H_n(q,p) \neq 0$ only in upper or lower half of the PSM like classical dynamics

Comparison of Wave Functions and Husimi Distributions of the QB and Massless NB

$\mu = 1$

$\mu = -1$

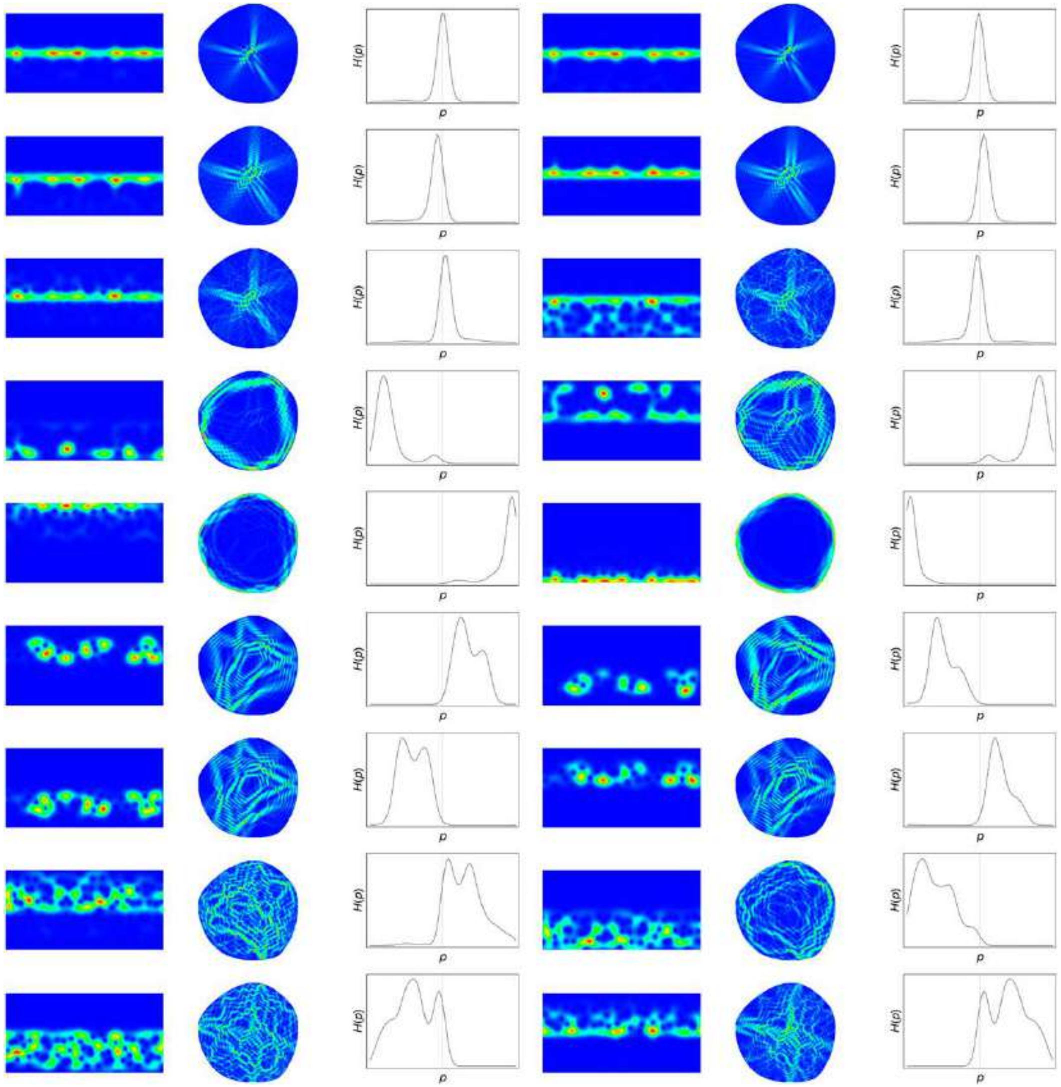

Located on small islands

Boundary condition:

$$\mathcal{K}\tilde{\psi}_2(\phi) = e^{i\phi}\mu\tilde{\psi}_1(\phi)$$

RMT Model for the Spectral Properties of Right Doublett Partner / Positive-p Husimi Partner

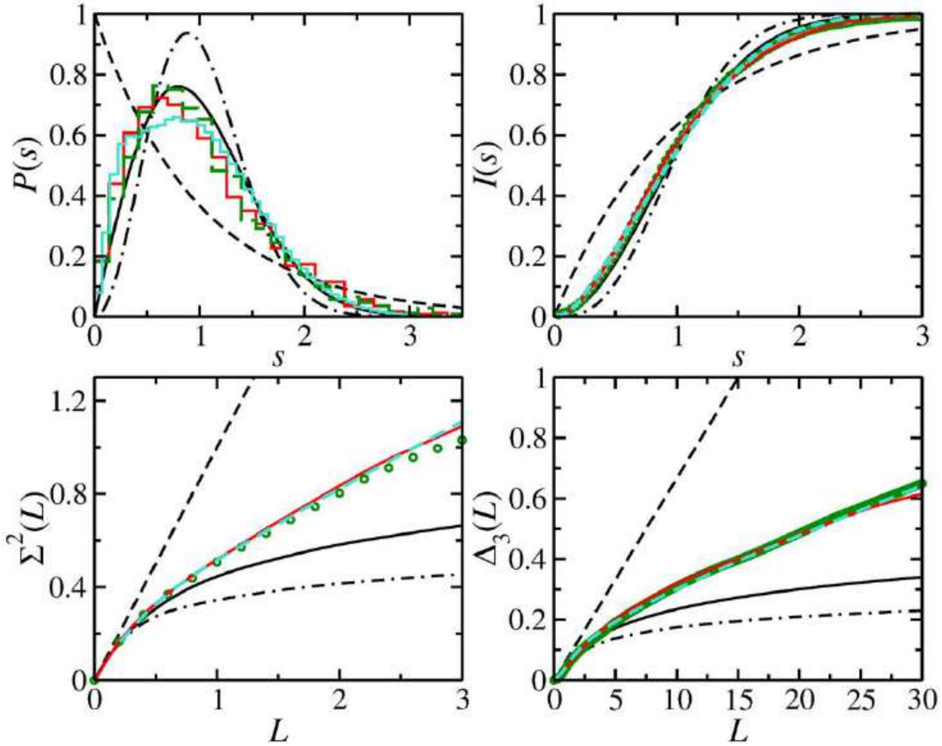

Green: QB

Red: Massless NB

Turquoise: RMT Model

τ_1=0.125

- RMT model: $$H^{mixed} = \begin{pmatrix} H & d_0\tau_1 V_1^\dagger \\ d_0\tau_1 V_1 & D_1 \end{pmatrix}$$

H : 300×300 GUE matrix

D_1: 100×100 diagonal Poisson matrix

- V_1 couples H (chaotic dynamics) to D_1 (regular dynamics) with the coupling τ_1 measured in units of mean spacing d_0

Length Spectra of the QB and Massless NB

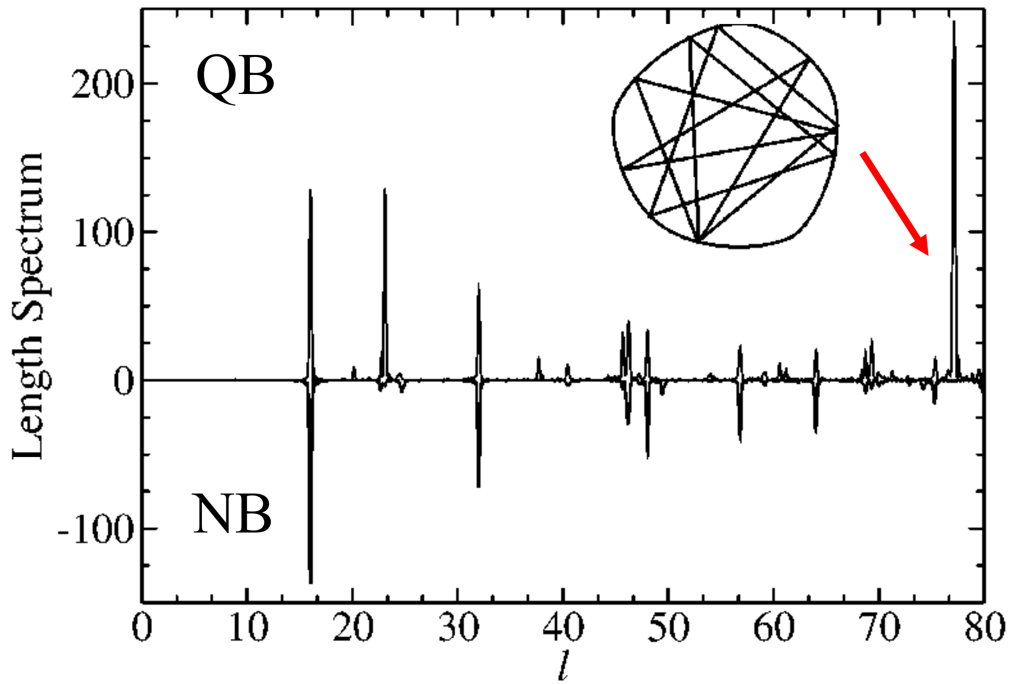

- The 'doublet partners' of the relativistic constant-width billiard are separated by several mean spacings $\rightarrow$ there is no dynamical tunneling
- Length spectra exhibit peaks at the lengths of the periodic orbits
- Peak at $l \cong 79$ corresponds to regular island in chaotic sea (11 bounces)

Thank you

for

your attention

Husimi Distribution of the First Wave Function Component of Half-Circle NB

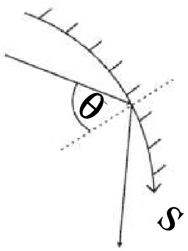

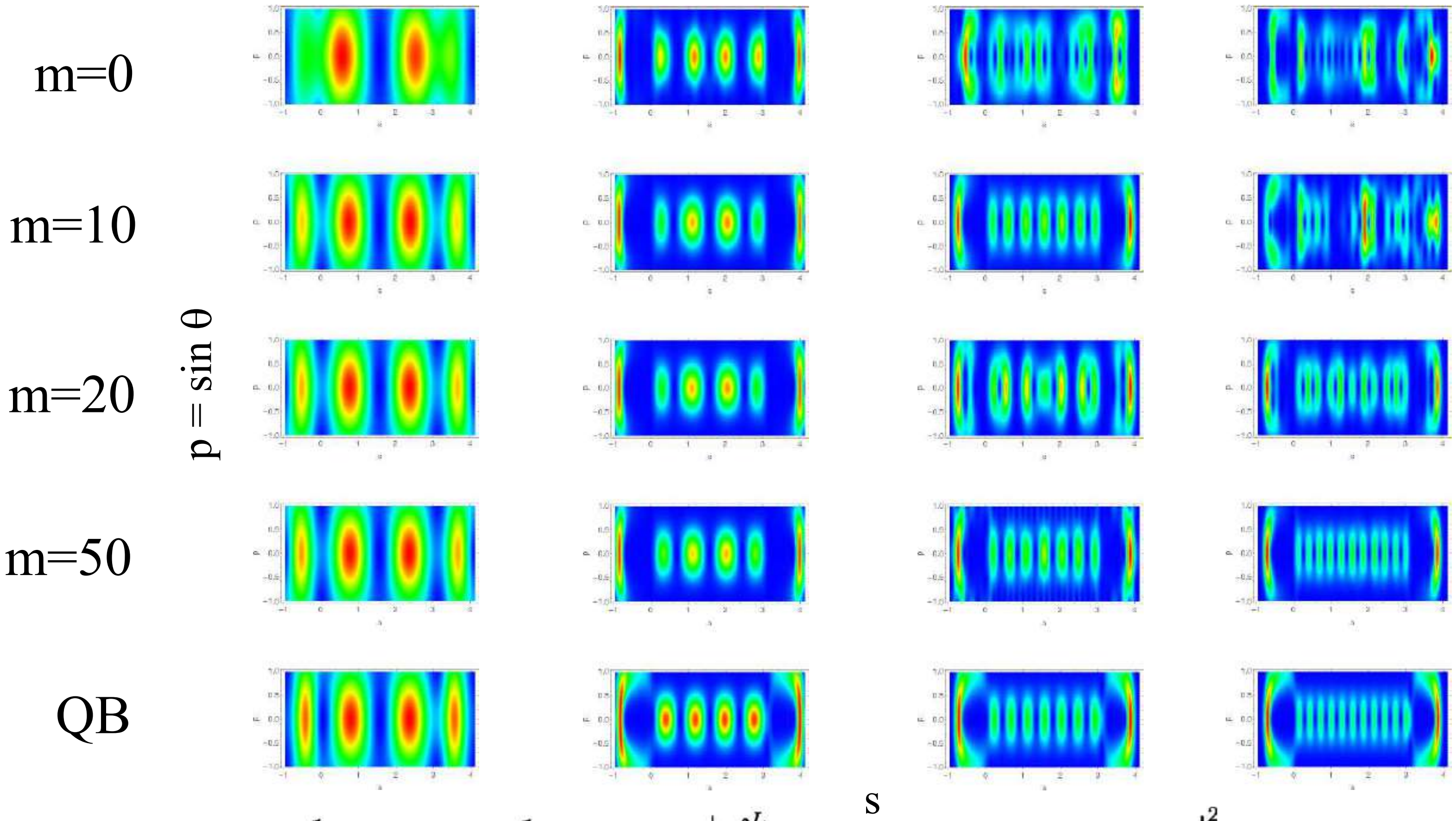

- Husimi functions $$H_n(p,q) = \frac{1}{2\pi k_n} \frac{1}{\int_0^L \mathrm{d}s \left| \left\langle \hat{n}(s), \vec{\nabla}\Psi_n(s) \right\rangle \right|^2} \left| \int_0^L \mathrm{d}s \left\langle \hat{n}(s), \vec{\nabla}\Psi_n(s) \right\rangle C^{\sigma}_{(p,q)}(s;k_n) \right|^2$$
- For m≈50 the Husimi distribution is close to that of the QB, for smaller mass it is similar to it for diameter-orbit like WFs

Spectral Properties of Robin Sector Billiard for Symmetric Case

- Robin BC

$$\left[\tilde{\beta} + \frac{1}{2}\kappa(s)\right] \Phi_j(s) + \partial_n \Phi_j(n,s)\big|_{n\to 0^-} = 0$$

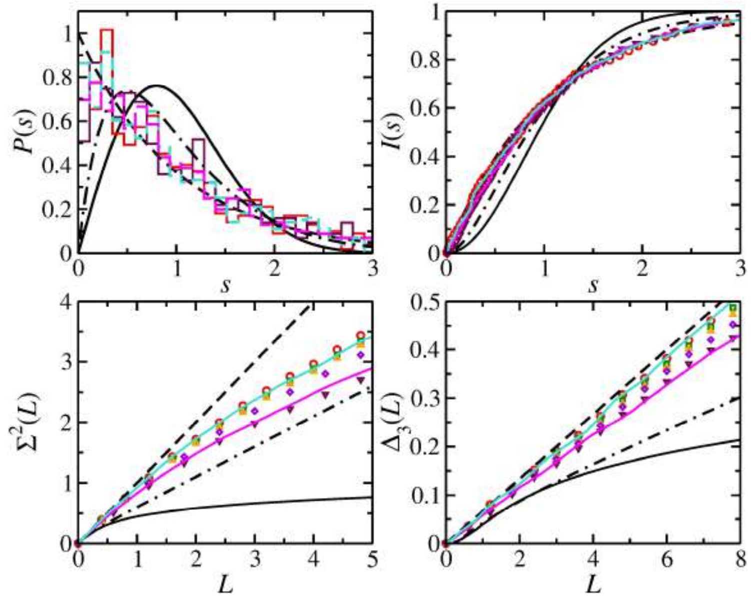

- Shown are the symmetric solutions

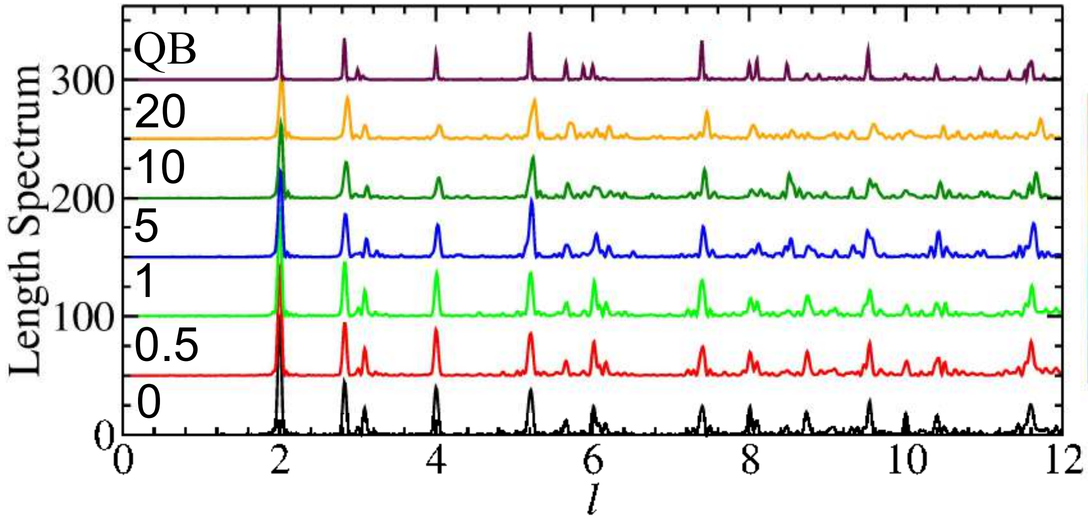

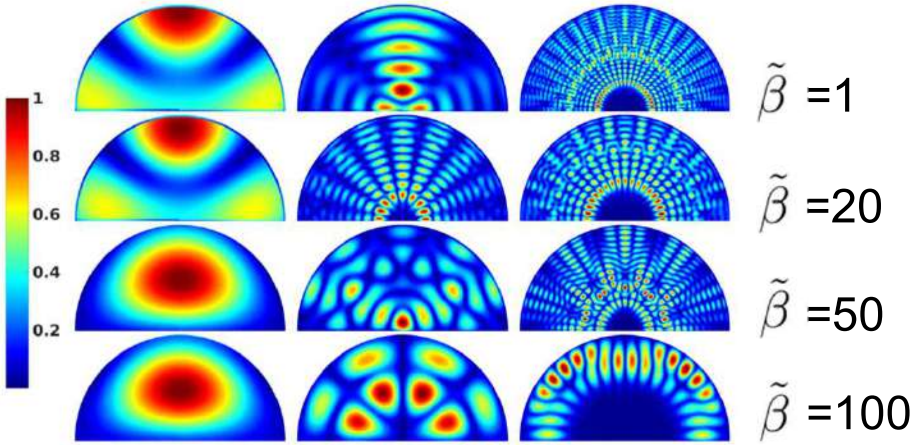

TBM Description for Graphene Billiards

- TBM for energies ω and eigenstates $|\Psi_{\vec{q}}(\vec{r})\rangle = \sum_j \left(C_A|\Phi_j^A\rangle + C_B|\Phi_j^B\rangle\right) e^{i\vec{q}\cdot\vec{R}_j}$

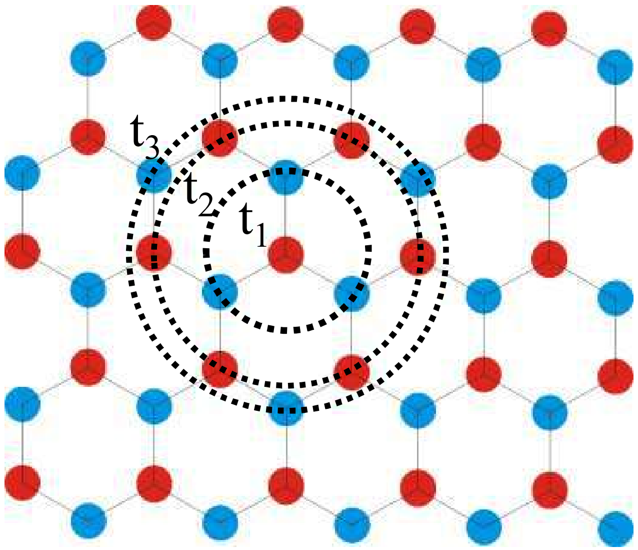

- Generalized eigenvalue problem

$$\mathcal{H}_{TB}|\Psi_{\vec{q}}(\vec{r})\rangle = \omega(\vec{q})\mathcal{S}_{WO}|\Psi_{\vec{q}}(\vec{r})\rangle$$

- Tight-binding Hamiltonian

$$\mathcal{H}_{TB} = \begin{pmatrix} f_0 + t_2 f_2(\vec{q}) & t_1 f_1(\vec{q}) + t_3 f_3(\vec{q}) \\ t_1 f_1(\vec{q}) + t_3 f_3(\vec{q}) & f_0 + t_2 f_2(\vec{q}) \end{pmatrix}$$

- Wavefunction overlap matrix

$$\mathcal{S}_{WO} = \begin{pmatrix} 1 + s_2 f_2(\vec{q}) & s_1 f_1(\vec{q}) + s_3 f_3(\vec{q}) \\ s_1 f_1(\vec{q}) + s_3 f_3(\vec{q}) & 1 + s_2 f_2(\vec{q}) \end{pmatrix}$$

- f_0 is resonance frequency of an “isolated“ void
- Nearest-neighbour contribution ~ t_1, s_1
- Next-nearest neighbour contribution ~ t_2, s_2
- Second-nearest neighbour contribution ~ t_3, s_3